Russian Chemical Reviews **75** (9) 749 – 763 (2006) © 2006 Russian Academy of Sciences and Turpion Ltd

DOI 10.1070/RC2006v075n09ABEH003625

A new class of compounds with unusual magnetic behaviour: quasi-one-dimensional complex oxides of the $A_{3n+3m}A'_nB_{3m+n}O_{9m+6n}$ family

G V Bazuev

Contents

I.	Introduction	749
II.	Commensurate and incommensurate oxides	750
III.	Low-dimensional platinum group metal oxides	752
IV.	Low-dimensional d and p element oxides	754
V.	Specific features of the formation of $A_{3n+3m}A'_nB_{3m+n}O_{9m+6n}$ oxides	757
VI.	Magnetic properties	757

Abstract. The results of investigations into the conditions of synthesis, structure and magnetic properties of quasi-one-dimensional perovskite-like complex oxides of the $A_{3n+3m}A'_n.B_{3m+n}O_{9m+6n}$ family (A = Ca, Sr, Ba; A′ = Cu, Ni, Co, Zn, Mg; B are platinum metals, Mn and other d and p elements) are generalised. It is shown that the low-dimensional structure of the compounds is determined by the presence of isolated chains consisting of octahedra occupied by the B cations and trigonal prisms with the A′-cations which alternate in various ratios. The reasons for the formation of incommensurate compounds and the methods for the refinement of their structures are considered. It is demonstrated that the presence of transition metals and the quasi-one-dimensional structure are responsible for the high anisotropy of the magnetic properties of the $A_{3n+3m}A'_nB_{3m+n}O_{9m+6n}$ oxides and, in particular, for the preservation of the intrachain exchange interactions to relatively high temperatures and the low temperatures of three-dimensional magnetic ordering. The bibliography includes 127 references.

I. Introduction

Over the recent years, compounds with low-dimensional crystal structures, in particular, two-dimensional layered and one-dimensional chain compounds manifesting strongly anisotropic physical properties have attracted much attention from specialists in inorganic and solid state chemistry and solid state physics. Among quasi-one-dimensional compounds with chain structures, complex platinum metal oxides, which effectively served as a basis for the emergence of this class of low-dimensional oxides, are of particular interest. Presently, a series of oxides with the general formula $A_{3n+3m}A'_nB_{3m+n}O_{9m+6n}$ based on such metals as Pt, Ir, Ru, Rh, *etc*. have been synthesised.[1,2] According to structural attributes, the Sr_4PtO_6 oxide[3] (that belongs to the K_4CdCl_6 structural type[4]), where both A and A′ cationic sites are occupied by Sr can be regarded as the first representative of this family. The values of *m* and *n* for this compound are 0 and 1, respectively.

G V Bazuev Institute of Solid State Chemistry, Urals Branch of the Russian Academy of Sciences, ul. Pervomayskaya 91, 620219 Ekaterinburg, Russian Federation. Fax (7-343) 374 44 95, tel. (7-343) 374 49 43, e-mail: bazuev@ihim.uran.ru

Received 25 January 2006
Uspekhi Khimii **75** (9) 835 – 850 (2006); translated by Ya V Zubavichus

Later in the 1990s, other oxides with the common formula $A_3A'BO_6$, where A = Ca, Sr, Ba; A′ = Cu, Ni, Zn, *etc*.; B are platinum group elements, were synthesised.[5–9] Noteworthy, it was complex oxide Sr_3CuPtO_6 that was the first reported compound from this series.[5,6] This new phase characterised by a distorted Sr_4PtO_6 structure with the Cu atoms substituting the Sr atoms in the positions A′ formed spontaneously upon an attempted growth of single crystals of strontium cuprate, a high-temperature superconductor, in a platinum crucible. More recently, oxides with formulas $A_4A'B_2O_9$ ($m = 1$ and $n = 3$), $A_6A'B_4O_{15}$ ($m = 1$ and $n = 1$) and $A_9A'_2B_5O_{21}$ ($m = 1$ and $n = 2$) and other compounds have been prepared.[10–12] A brief analysis of the conditions of synthesis and description of the structures of compounds from this class synthesised prior to 2000 can be found elsewhere.[13]

In structural inorganic chemistry, the above oxides are typically considered as perovskite-related, since complex oxides with the common formula ABO_3 can formally be regarded as a particular case of the formula $A_{3n+3m}A'_nB_{3m+n}O_{9m+6n}$ (for $m = 1$ and $n = 0$). The perovskite structure is usually described in one of two ways. On the one hand, the perovskite structure can be represented as a spatial network of polyhedra, *viz*., BO_6 octahedra, which can be picked out based on the mutual arrangement of the metal and oxygen atoms constituting the compound. This polyhedral representation is especially pictorial and convenient for the analysis of various structural distortions of perovskites related to the rotation or tilting of the octahedra. The ideal cubic perovskite structure in the polyhedral representation is depicted in Fig. 1 *a*.

On the other hand, a description of the perovskite structure can be based on the concept of cubic and hexagonal close packings of the atoms A and O constituting an ABO_3 perovskite. Strictly speaking, only the cubic close packing refers to the perovskite structure. The hexagonal close packing is typical of crystal structures of some other compounds with the same stoichiometry (*e.g*., $BaNiO_3$,[14] see Fig. 1 *b*) or with several structural modifications [including $BaMnO_3$ (Refs 15 and 16)]. For some of ABO_3 oxides (in particular, for $BaTiO_3$)[17] both perovskite and hexagonal modifications are known. Taking these factors into account, the hexagonal perovskite structure can be represented as a stack of closely packed AO_3 layers along the *c* axis (Fig. 2) with the B atoms occupying the octahedral cavities formed by the oxygen anions. The A cations are close in size to the O^{2-} oxygen anions, whereas the B cations are characterised by a smaller radius. According to the stoichiometry, the number of the octahedra is equal to the number of the A atoms. Chains (columns) composed

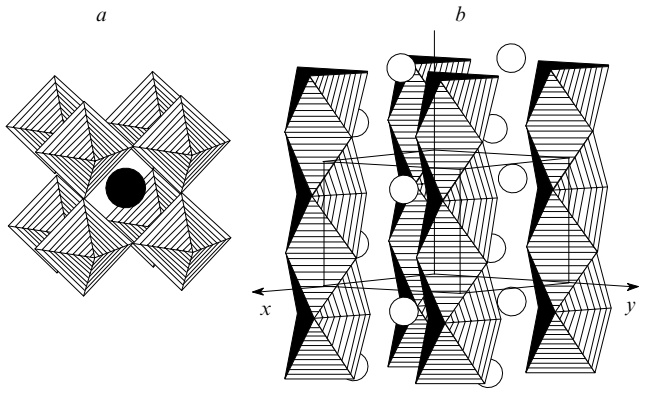


Figure 1. The cubic (*a*) and hexagonal (*b*) structures of an ABO_3 perovskite.

of face-sharing octahedra are characteristic of the crystal structure of the 2H polytype of an ABO_3 perovskite (see. Fig. 1 *b*).

An analysis of the structure of complex oxides belonging to the $A_{3n+3m}A'_nB_{3m+n}O_{9m+6n}$ family taking into account the stacking sequence of closely packed AO_3 layers (see Fig. 2 *a*) reveals its close relation to the hexagonal perovskite structure. For this purpose, it is convenient to triple the perovskite formula unit to $A_3B_3O_9$ and represent the composition of a layer with the hexagonal close packing as A_3O_9. Then the structure of a compound belonging to the family $A_{3n+3m}A'_nB_{3m+n}O_{9m+6n}$ can be considered as a stack of layers with stoichiometries A_3O_9 and $A_3A'O_6$ along the *c* axis. The $A_3A'O_6$ layers can formally be generated from the A_3O_9 layers by replacing three oxygen atoms with an A′ atom. The ratio between the number of $A_3A'O_6$ and A_3O_9 layers is determined by the n/m ratio in the formula $A_{3n+3m}A'_nB_{3m+n}O_{9m+6n}$. The presence of the $A_3A'O_6$ layers in the oxide structures gives rise to a new type of coordination, additional to the octahedral one, *viz*., trigonal prismatic (Fig. 2 *b*). The unit cell parameter *a* for these compounds relates to the respective parameter of the hexagonal perovskite lattice as $a = \sqrt{3}a_p \approx 10$ Å, whereas the parameter *c* depends on *m* and *n*. A change in the composition of the oxides from ABO_3 to $A_{3n+3m}A'_nB_{3m+n}O_{9m+6n}$ gives rise to the emergence of chains composed of alternating octahedra and trigonal prisms going along the *c* axis. This structure is typical, for instance, of Sr_4PtO_6, where one out of four Sr atoms occupies a trigonal prismatic site (Fig. 3). In the $A_3A'BO_6$ oxides, the octahedra are occupied by the B cations, whereas the trigonal prisms are occupied by the A′ cations. Evidently, the ratio between the number of prisms and octahedra in the structure is determined by the ratio of stoichiometric coefficicents of the A′ and B atoms in the formula. For instance, an $A_4A'B_2O_9$ oxide includes one prism per two octahedra and thus contains chains composed of dimers of octahedra

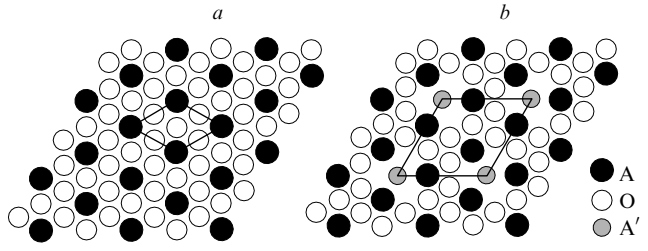


Figure 2. Compositions of alternating layers in oxides of the $A_{3n+3m}A'_nB_{3m+n}O_{9m+6n}$ family for two ultimate stoichiometries.
(*a*) A_3O_9 ($n = 0, m = 1$), (*b*) $A_3A'O_6$ ($n = 1, m = 0$). The unit cells in the *ab* plane are shown.

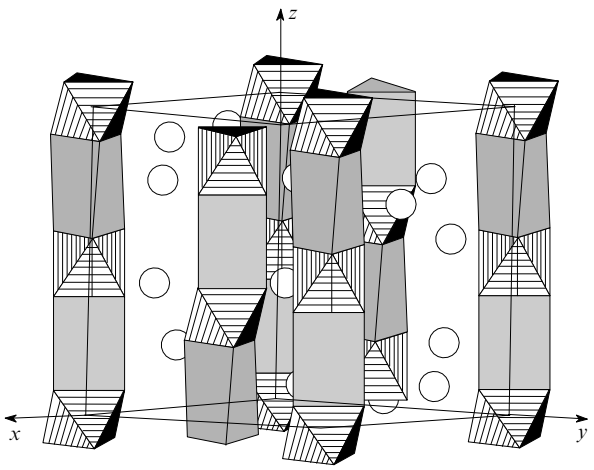


Figure 3. The crystal structure of Sr_4PtO_6.
The octahedra are occupied by the Pt atoms, the trigonal prisms are occupied by the Sr atoms; open circles denote the Sr atoms that separate the Sr – Pt-chains.

separated by a trigonal prism. In the structure of an $A_9A'_2B_5O_{21}$ oxide, the chains are formed by dimers and trimers of the BO_6 octahedra separated by an $A'O_6$ prism (Fig. 4).[18] The octahedra are connected to each other and to the prisms through face-sharing, which gives rise to rather short metal – metal distances. In these structures, the chains are isolated from each other by the A cations (most frequently, alkaline-earth metals).

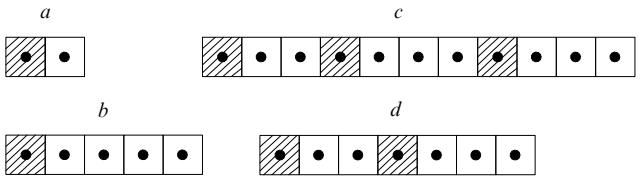


Figure 4. A schematic representation of the chain composition for some oxides of the $A_{3n+3m}A'_nMn_{3m+n}O_{9m+6n}$ family.[18]
(*a*) $A_3A'MnO_6$, (*b*) $A_6A'Mn_4O_{15}$, (*c*) $A_{14}A'_3Mn_8O_{11}$, (*d*) $A_9A'_2Mn_5O_{21}$. Shaded squares denote trigonal prisms, plain squares denote octahedra.

II. Commensurate and incommensurate oxides

Following the synthesis of some representatives of the $A_{3n+3m}A'_nB_{3m+n}O_{9m+6n}$ family as polycrystalline powders, the frequent formation of incommensurate structures was discovered.[10, 11, 19] The incommensurability of the oxides is caused by such factors as their quasi-one-dimensional structure, different composition of the $[A]_\infty$ and $[(A',B)O_3]_\infty$ chains and relatively easily occurring inversion of cations over the polyhedral sites in the chains. The crystal structure of a compound is regarded as incommensurately modulated along the *c* axis provided that the ratio between the translation periods of the two chains is irrational.

Crystal structures of these compounds can be considered as a composite of two interacting subsystems characterised by identical unit cell parameters *a* and *b* but different parameters *c*, *i.e*., c_1 and c_2. The first subsystem includes the $[(A',B)O_3]_\infty$ chains with the parameter $c_1 \approx c_{\text{hex.per.}}/2$, which defines the mean distance between the cations within the polyhedral chains. The second subsystem is composed of the $[A]_\infty$ chains with the parameter $c_2 = c_{\text{hex.per.}}$, which defines the mean distance between alternating

A_3O_9 and $A_3A'O_6$ planes. Therefore, the ratio of the translation parameters c_1 and c_2 corresponding to the two mean sublattices is directly related to the stoichiometry. If the c_1/c_2 ratio (the so called γ-component of the modulation vector) is rational, the structure is regarded as commensurate; but if the ratio is irrational, the translation vector along the c axis becomes formally infinite and thus the structure should be regarded as incommensurate.

Therefore, for a commensurate unit cell, $pc_1 = qc_2$, *i.e.*, $c_1/c_2 = q/p$ (q and p are integers). A unit cell of an oxide of the $A_{3n+3m}A'_nB_{3m+n}O_{9m+6n}$ family consists of $2p$ A_3O_9 and/or $A_3A'O_6$ layers and q polyhedra.[12] {Within this model, the c_1 parameter refers to the $[A]_\infty$-subsystem and the c_2 parameter refers to the $[(A',B)O_3]_\infty$ subsystem.} Each A_3O_9 layer occupies one octahedral site within the chain. Upon the introduction of an $A_3A'O_9$ layer, a prismatic site is generated, which is twice as large as the octahedral site.

Let us consider two ultimate compositions of oxides from the $A_{3n+3m}A'_nB_{3m+n}O_{9m+6n}$ family, *viz.*, ABO_3 ($n = 0$, $m = 1$) and $A_3A'BO_6$ ($n = 1$, $m = 0$). A unit cell of a 2H-perovskite ABO_3 contains two A_3O_9 layers and two transition metal cations, thus $p = 1$, $q = 2$, $c_1/c_2 = 2$. Meanwhile, the structure of an $A_3A'BO_6$ oxide includes 6 layers (3 A_3O_9 layers and 3 $A_3A'O_6$ layers) and 4 cations per unit cell, *i.e.*, $p = 3$, $q = 4$, $c_1/c_2 = 4/3$. These two limiting cases demonstrate that $(4p/3) \leqslant q \leqslant 2p$. For commensurate oxides with the stoichiometry $A_4A'B_2O_9$, $p = 2$, $q = 3$ and $c_1/c_2 = 3/2$, whereas $p = 3$, $q = 5$ and $c_1/c_2 = 5/3$ for the $A_6A'B_4O_{15}$ oxides. As has been shown by Blake *et al.*,[12] an analysis of stacking sequences of the $A_3A'O_6$ and A_3O_9 layers based on the parameters p and q allows one to predict possible stoichiometries of compounds from the $A_{3n+3}A'_nB_{3+n}$. $.O_{9+6n}(m = 1) \equiv (A_3A'O_6)_n(A_3O_9)$ family and, furthermore, establish criteria for their commensurability.

One compound can have both commensurate and incommensurate modifications. (However it should be kept in mind that these modifications would correspond to different, although quite similar, compositions.) The literature data on the conditions of formation of commensurate and incommensurate phases are somewhat self-contradicting. For instance, $Sr_4CuIr_2O_9$ phases with commensurate and incommensurate structures were prepared by the calcination of reactants in air at the same temperature of 1120 °C for 5 h and 4 days, respectively.[10] A complex oxide Sr_3ZnRhO_6 as a commensurate phase was synthesised from Sr carbonate, Zn oxide and Rh metal by the calcination in a Pt crucible in air first at 800 °C for 10 h and then at 1150 °C for 3 days.[20] Meanwhile, the thermal decomposition of the respective metal nitrates at 450 °C for 24 h followed by the calcination at 1150 °C for 3 days yielded the incommensurate phase. The authors speculated that it is a prolonged thermal treatment that is responsible for the formation of incommensurate phases. The transition from the commensurate to the incommensurate phase is realised in a narrow temperature range. As has been suggested,[21] the transition is irreversible. Information on the chemical composition of the commensurate and incommensurate phases is also ambiguous. According to results by Battle *et al.*,[10] compositions of the two phases of $Sr_4CuIr_2O_9$ are indistinguishable within the error limit, whereas the incommensurate phase of $Sr_3ZnRhO_{6+\delta}$ was found to be richer in oxygen than its commensurate modification. Layland and zur Loye reported[20] that the Sr_3MRhO_6 oxide is extremely sensitive to fine details of the synthesis conditions (such as changes in the oxygen partial pressure, heating rate, temperature, duration, *etc.*), as evidenced by the emergence of the incommensurate phase. It is of note that the c_1/c_2 ratio can vary continuously during the thermal treatment. Moore and Battle argued[22] that the composition of the starting load for the synthesis of $Sr_4CuMn_2O_9$ in the commensurate modification should be changed from the stoichiometric 4 : 1 : 2 (Sr : Cu : Mn) to 4 : 1.04 : 1.92.

It may well be suggested that any compound (either with a commensurate or incommensurate structure) is characterised by unique composition and intrinsic structural peculiarities. The formation of incommensurate structures can be due to the insertion of oxygen into trigonal prisms giving rise to two octahedra instead of a prism, generation of vacancies and changes in the chain length (*i.e.*, the c_1 parameter).

In principle, usual three-dimensional space groups can be used for the interpretation of incommensurate structures, but this requires the postulation of superstructures characterised by extremely large unit cells, which complicates their analysis. In particular, a structural description of an incommensurate phase of the $Sr_{1.3244}Cu_{0.3244}Mn_{0.6756}O_3$ oxide would require a c parameter as large as 191.92 Å.[21]

In practice, it is much more convenient to describe such crystal structures within the so-called superspace formalism with space groups of a higher dimensionality.[2, 19] For this purpose, additional coordinates associated with a shift of the modulation wave with respect to the parent structure by a vector d are introduced. The dimensionality of this new space is given by 3 + d, where d is the number of linearly independent modulation vectors $\boldsymbol{q}$. In the reciprocal space, the modulation vector $\boldsymbol{q}$ is defined as:

$$\boldsymbol{q} = \alpha\boldsymbol{a}^* + \beta\boldsymbol{b}^* + \gamma\boldsymbol{c}^*,$$

where α, β and γ are components of the vector $\boldsymbol{q}$; $\boldsymbol{a}^*$, $\boldsymbol{b}^*$ and $\boldsymbol{c}^*$ are the reciprocal unit cell parameters of the unmodified phase.

In the case of $A_{3n+3m}A'_nB_{3m+n}O_{9m+6n}$ oxides, the incommensurability can occur only in one direction, *viz.*, along the c axis, thus $\boldsymbol{q} = \gamma\boldsymbol{c}^*$ and the structure is described in the space of dimensionality (3 + 1).

Four basis vectors are required to index all diffraction lines of a modulated phase

$$\boldsymbol{H} = h\boldsymbol{a}_1^* + k\boldsymbol{b}_1^* + l\boldsymbol{c}_1^* + m\boldsymbol{c}_2^*,$$

where $\boldsymbol{H}$ is the diffraction vector in the reciprocal space. The 'principal' reflections ($hkl0$) with $l \neq 0$ and ($hk0m$) with $m \neq 0$ can be interpreted neglecting the modulation as Bragg reflections corresponding to the $[(A',B)O_3]$ and [A] subsystems, respectively. In such a case, the diffraction pattern manifests no satellite reflections ($hklm$) with $l \neq 0$ and $m \neq 0$. If the two subsystems are mutually ordered, the satellite reflections appear imposed on the main set of principal reflections.

Sometimes, differences in the chemical composition of commensurate and incommensurate phases are so small that they cannot be determined by analytical techniques. To overcome this problem, a model was elaborated within the superspace formalism, which makes it possible to accurately determine the stoichiometry of an $A_{3n+3m}A'_nB_{3m+n}O_{9m+6n}$ oxide based on its X-ray diffraction parameters. For this purpose, the formula of a compound should be rewritten as $A_{1+x}A'_xB_{1-x}O_3$ [$x = n/(3m + 2n)$], since x can be directly related to the γ-component of the modulation vector[2, 19]

$$\gamma = \frac{c_1}{c_2} = \frac{c_2^*}{c_1^*} = \frac{1+x}{2}.$$

The γ value can vary from 0.5 to 0.75, which corresponds to variations in x over a range of $0 \leqslant x \leqslant 0.5$. Within this model, x can change continuously, which corresponds to various combinations of octahedra and trigonal prisms in the chain and gives rise to the infinite number of possible unique structures and chemical compositions. Oxides with stoichiometries from ABO_3 to $A_3A'BO_6$ fall into this range. As has been mentioned above, the ratio between the number of prisms and octahedra in the chain is determined by the ratio between the number of atoms A′ and B

$$\frac{N_{\text{prism}}}{N_{\text{oct}}} = \frac{x}{1-x}.$$

Therefore, if the c_1/c_2 ratio is known, the value of x can be determined from the above expression with a high accuracy, which is equivalent to the precise knowledge of stoichiometry for an $A_{3n+3m}A'_nB_{3m+n}O_{9m+6n}$ oxide. This implies that a compound

$A_{1+x}A'_xB_{1-x}O_3$ can be considered as incommensurate or commensurate provided that x is irrational or rational, respectively.

Atomic density modulation functions for compounds of this family can be described within the superspace formalism with sawtooth functions of occupancies and modulations of shifts along the c axis. The major advantage of the use of sawtooth shift modulation functions is the significant decrease in the number of independent variables describing the structure. By varying the parameters, compounds with any stoichiometries (or with any values of x), including ultimate ones, such as 2H-perovskite ABO_3 ($x = 0$) or $A_3A'BO_6$ ($x = 0.5$), can be represented.

In a structural study of an incommensurate phase of $Sr_{1+x}Cu_xMn_{1-x}O_3$ ($x = 1/3$),[21] the Bragg peaks observed in the experimental diffraction pattern were initially indexed based on two sublattices: [(Cu, Mn)O_3] in the space group $R\bar{3}m$ and [Sr] in the space group $P\bar{3}c1$ (Fig. 5) with similar a parameters and different c parameters, *i.e.*, c_1 and c_2. The c_1/c_2 ratio was found to be 0.6625, which clearly indicated the incommensurability of the phase (a ratio 0.66_6 and $x = 0.3250$ are expected for the respective commensurate oxide with a similar composition). The refinement in the superspace group $R\bar{3}m(00\gamma)0s$ yielded the precise stiochiometry ($x = 0.3244$) and unit cell parameters $a = 9.5933(7)$ Å, $c_1 = 2.5933(3)$ Å and $\gamma = 0.6622(1)$. The stoichiometry determined differ from $Sr_4CuMn_2O_9$ by an increased Mn/Cu ratio and a larger number of octahedral sites in the chains going along the c axis. The elementary unit of the chain includes 11 combinations (1 TP + 2 O) and one combination (1 TP + 3 O), where TP means trigonal prism and O means octahedron.

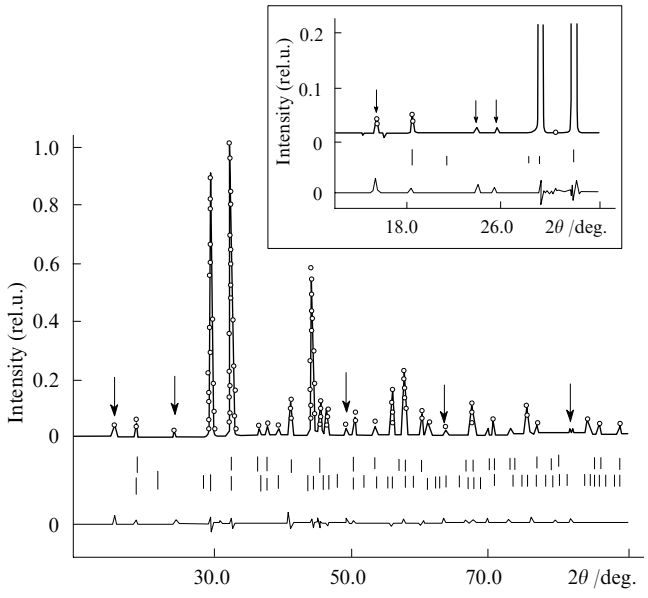


Figure 5. The Rietveld refinement of the powder pattern for a composite oxide, $Sr_{1.3244}Cu_{0.3244}Mn_{0.6756}O_3$: experimental data (dots), best-fit and difference.[21]
The positions of reflections indexed for two independent sublattiches in 3D-space groups are marked with dashes; non-indexable reflections are marked with arrows.

The results reported by Abakumov *et al.*[23] and by Mironov *et al.*[24] can be cited as an illustrative example on the structure determination of a quasi-one-dimensional oxide, $Sr_{1.32}.Mn_{0.83}Cu_{0.17}O_3$, using a combination of techniques, including electron diffraction, high-resolution electron microscopy and X-ray diffraction coupled with the crystal structure refinement in the (3 + 1)D-space. The experimentally found value of γ for this compound was 0.6616(1), which corresponds to $x = 0.3232$ in $A_{1+x}A'_xB_{1-x}O_3$. This value is close to the ratio $p'/q' = 1/3$, where p' is the number of prisms in the chain and the number of octahedra is $q'-p'$ (see †). Taking into account that $x = p'/q'$, this may be rewritten as

$$\frac{N_{\text{prism}}}{N_{\text{oct}}} = \frac{x}{1-x} = \frac{p'}{q'-p'}.$$

Based on this expression, the sequence of octahedra and prisms in the chain was determined. According to the Farey's rule,[2] a sequence with the most uniform distribution of trigonal prisms is realised in the chain of polyhedra. Therefore, the ratio p'/q' for $x = 0.3232$ should be 32/99. This implies that the chain of polyhedra going along the c axis contains 99 polyhedra representing dimers and trimers of octahedra separated by single trigonal prisms. The overall parameter c appears close to 515 Å, which makes a traditional description of the structure in the 3D-approximation impossible. In contrast to the $Sr_{1.3244}Mn_{0.6756}Cu_{0.3244}O_3$ phase discussed above,[21] the trigonal prismatic sites in $Sr_{1.32}Mn_{0.83}Cu_{0.17}O_3$ are occupied by the Cu and Mn cations $[Sr_{1.323}(Cu^{2+}_{0.174}Mn^{2.27+}_{0.149})_{\text{prism}}(Mn^{4+}_{0.677})_{\text{oct}}O_3]$ (Ref. 23).

The X-ray diffraction pattern of $Sr_3ZnRhO_{6.34}$ can be indexed[20] assuming two sublattices with $a = 9.6378(5)$ Å and $c = 2.7012(2)$ Å in the space group $R3m$ and with $a = 5.5640(9)$ Å and $c = 3.9539(7)$ Å in the space group $P31c$. For this phase, the ratio $c_1/c_2 = 0.6832$ is significantly smaller than the ideal value 3/4 expected for the commensurate phase Sr_3ZnRhO_6. On the other hand, this value is close to 2/3 typical of structures comprising two octahedra and one trigonal prism along the c axis. Such a structure corresponds to the composition $A_4A'B_2O_9$. The increased oxygen content in the incommensurate phase can indicate the transformation of trigonal prisms into octahedra upon the respective synthesis conditions. Stitzer *et al.*[13] noted that it should be possible to detect such a transition using the thermogravimetric analysis, although no experimental evidence of the process has been reported so far. Presently, the conditions of synthesis favouring the formation of the above oxides with either commensurate or incommensurate structures remain unclear.

III. Low-dimensional platinum group metal oxides

1. $A_3A'BO_6$ oxides

Platinum metals form an extended series of quasi-one-dimensional oxides with the common stoichiometry $A_3A'BO_6$. Oxides with other compositions have also been reported. Selected examples of these compounds are listed in Table 1. A systematic analysis indicates that the platinum group metals in the quasi-one-dimensional $A_3A'BO_6$ oxides can be in the tri- (Rh), tetra- (Rh, Pt, Ir or Ru) and pentavalent (Ru, Ir or Rh) states. It is of note that complex Rh^{5+} oxides from this family (*e.g.*, Sr_3NaRhO_6 and Sr_3LiRhO_6) were the first examples of rhodium oxides in the formal oxidation state 5+ (see Ref. 53). These compounds were synthesised at 600 °C by the crystallisation of a melt of RhO_2, $Sr(OH)_2$ and alkali metal hydroxides at ambient pressure. These compounds manifest low stability in air. Upon their storage in a humid atmosphere, Rh^{5+} undergoes partial reduction to Rh^{4+}.

The A′ sites can be occupied by alkali metals, 3d elements (most typically, bivalent), Cd, Mg and rare-earth elements. The vast majority of $A_3A'BO_3$ oxides (B = Pt, Ir, Rh, Ru) are isostructural to Sr_4PtO_6. The Sr_4PtO_6 oxide is crystallised in the rhombohedral space group $R\bar{3}c$ with $a = 9.740(2)$ Å and $c = 11.900(2)$ Å (in the hexagonal setting). A similar structure is also typical of Ca_4PtO_6 (Refs 25 and 26) and Ba_4PtO_6 (Ref. 30). The unit cell parameters of these oxides are somewhat modified as compared to the aforementioned values of the Sr^{2+} compound according to the ionic radii of Ca^{2+} and Ba^{2+}.

† The parameters p' and q' relate to the aforementioned parameters p and q through the following expressions: $p' = 2p-q$, $q' = q$.

Table 1. Chemical compositions of oxides of the $A_{3n+3m}A'_nB_{3m+n}O_{9m+6n}$ family (B is a platinum group metal).

m	*n*	Gross formula	Compound
1	0	ABO_3	$BaNiO_3$ (Ref. 14)
0	1	$A_3A'BO_6$	Ca_4PtO_6,[25,26] Ca_4IrO_6,[27] Ca_4PdO_6,[28] Sr_4PtO_6,[3] Sr_4IrO_6,[27] Sr_4PdO_6,[28] Sr_4RhO_6,[29] Ba_4PtO_6,[30] $Ca_{3.5}Cu_{0.5}PtO_6$,[31] $Sr_3A'PtO_6$ (A′ = Cu,[5,6] Ni,[32] Co,[33] Zn, Cd,[34] Mg[35]), $(Na,La_2)NaPtO_6$,[36] $Ca_3A'IrO_6$ (A′ = Na,[37] Co,[38] Cu,[39] Ni,[40] Zn,[41] Mg[41]), $Sr_3A'IrO_6$ (A = Li, Na, Ca, Co, Ni, Zn Cu, Cd, Mg),[7,42–45] Ba_3NaIrO_6,[46] $A_3A'RuO_6$ (A = Ca, Sr, Ba; A′ = Li, Na,[9,35,45–47] Co,[38] Cu[48]), $Ca_3A'RhO_6$ (A′ = Co, Fe),[49] $Sr_3A'RhO_6$ (A′ = Zn,[20] Ni, Cu,[50] Sc, In, Sm–Yb, Y[51,52]), Sr_3ARhO_6 (A = Li, Na)[53]
1	3	$A_4A'B_2O_9$	$Sr_4Ru_2O_9$,[54] $A_4A'Ir_2O_9$ (A = Sr, Ba; A′ = Cu, Zn)[10]
2	3	$A_5A'B_3O_{12}$	$Ba_5CuIr_3O_{12}$ (Ref. 12)
1	1	$A_6A'B_4O_{15}$	$Ba_6A'Ir_4O_{15}$ (A′ = Cu, Zn),[11] $Sr_6Rh_5O_{15}$ (Ref. 55)
5	3	$A_8A'B_6O_{21}$	$Ba_8CoRh_6O_{21}$ (Ref. 56)
1	2	$A_9A'_2B_5O_{21}$	$Ba_9Cu_2Ir_5O_{21}$,[12] $Ba_9Rh_8O_{21}$ (Ref. 57)
3	1	$A_{12}A'_9B_2O_{33}$	$Ba_{12}Rh_{9.25}Ir_{1.75}O_{33}$ (Ref. 58)
5	9	$A_{14}A'_3B_8O_{33}$	$Ba_{14}Cu_3Ir_8O_{33}$ (Ref. 12)
7	9	$A_{16}A'_3B_{10}O_{39}$	$Ba_{16}Cu_3Ir_{10}O_{39}$ (Ref. 12)

Oxides containing divalent copper in the A′ sites (in particular, Sr_3CuPtO_6, Sr_3CuIrO_6, Ca_3CuIrO_6 and Ca_3CuRhO_6) are characterised by slightly different structures due to the Jahn–Teller nature of the Cu^{2+} cation. The change is due to a shift of the Cu^{2+} cation from the centre of the trigonal prism towards one of its rectangular faces. As a result, the symmetry lowers from rhombohedral to monoclinic (space group $C2/c$). The crystal structure of a monoclinic modification of the $Ca_{3.1}Cu_{0.9}RuO_6$ oxide is shown in Fig. 6. Interestingly, the presence of calcium cations in the trigonal prismatic sites does not increase the symmetry of the phase and both the Ca^{2+} and Cu^{2+} ions in the prismatic sites are actually located in one of the faces adopting the planar square coordination.

The A sites in the $A_3A'BO_6$ oxides are preferably occupied by alkaline-earth metals. The only exception to this rule is represented by the $(Na,La_2)NaPtO_6$ oxide, where La and Na jointly occupy the A sites. A half of Na^+ cations in this strucure occupy the trigonal prismatic sites.

2. Oxides with other stoichiometries

A number of platinum group metal oxides corresponding to other *n* and *m* have been synthesised, which are characterised by a larger ratio of the number of octahedral sites to that of prismatic sites than in $A_3A'BO_6$ (see Table 1). Among them, $Sr_4Ru_2O_9$ is worth mentioning, since a quasi-one-dimensional structure with empty trigonal prisms is known for this compound.

An increase in the fraction of octahedra in the chain gives rise to an increase in *c*. For instance, *c* is 35.0564 Å for $Ba_{16}Cu_3Ir_{10}O_{39}$. Such oxides are characteristic of two metals, *viz*., Ir and Rh, with one exception represented by $Ba_4Pt_{1.7}Cu_{1.1}O_x$. This phase was obtained in an attempted growth of single crystals of $ErBa_2Cu_3O_7$, a high-temperature superconductor, in a platinum crucible.[59] The structural studies of these objects are complicated by the necessity to refine a large number of positional parameters. Nevertheless, the structure of

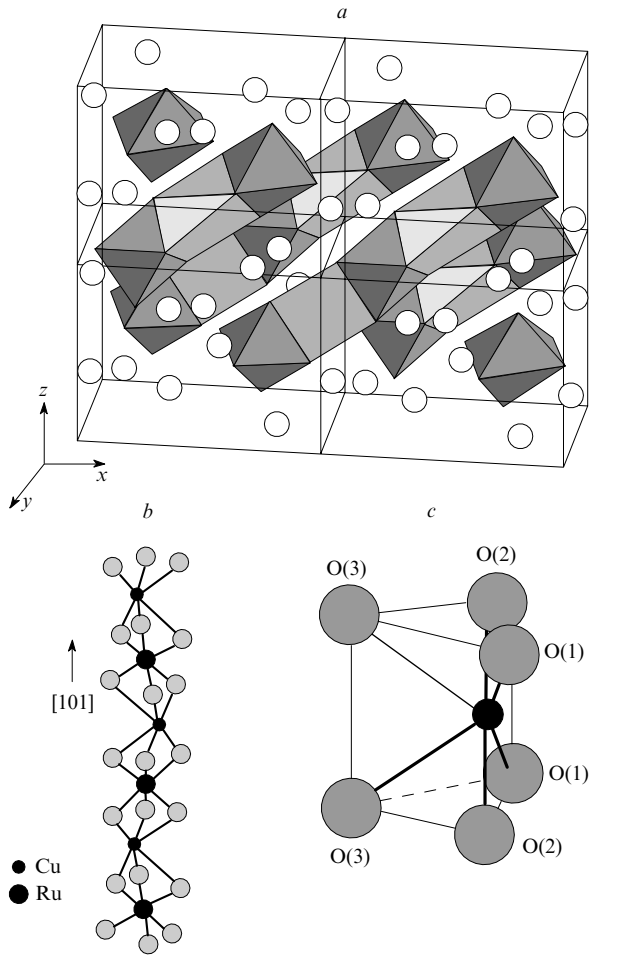


Figure 6. The crystal structure of $Ca_{3.1}Cu_{0.9}RuO_6$.[48] The orientation of chains of polyhedra in the monoclinic unit cell (*a*), the arrangement of atoms within a chain (*b*) and the expanded view of a trigonal prismatic site (*c*) are shown.

$Ba_{16}Cu_3Ir_{10}O_{39}$ with 54 independent atoms in a unit cell‡ was successfully refined based on the neutron diffraction data.[12]

As a rule, only small plate-, needle- or rod-like single crystals of $A_{3n+3m}A'_nB_{3m+n}O_{9m+6n}$ oxides (A = Ca, Sr, Ba; A′ = Cu, Ni, Co, Zn, Mg; B is a platinum group metal, Mn, *etc*.) can be grown. The vast majority of single crystals was grown from various fluxes composed of metal carbonates, hydroxides, halides or their eutectic mixtures. Alkaline-metal carbonates, metals, simple or pre-prepared complex oxides with a specific composition were used as reactants. The syntheses were conducted in aluminium, platinum, silver or nickel crucibles in air or in sealed ampules (as in the case of Sr_3NaIrO_6, see Ref. 43). In particular, single crystals of $Ba_8CoRh_6O_{21}$ were grown[56] from a potassium carbonate flux in an alumina crucible starting from Rh, $BaCO_3$ and Co_3O_4 powders. The loaded crucible was heated in air from room temperature to the reaction temperature of 1050 °C at a rate of 600 °C h^{-1}, kept at this temperature for 12 h and cooled down to 875 °C at a rate of 12 °C h^{-1}. Then the furnace was switched off and the crucible with the reaction product was left inside the furnace to slowly cool down. The flux was removed by washing with water, and the crystals were withdrawn from the crucible. Single crystals of $Sr_{14}Cu_3Mn_8O_{33}$ were synthesised in a similar way (the annealing at 1200 °C for 48 h followed by cooling down to 880 °C at a rate of 6 °C h^{-1}).[21]

‡ To our knowledge, this is the most complex structure among this class of oxides solved and refined from powder diffraction data.

Relatively large single crystals were obtained using the method of crystal growth from salt melts. This enabled high-precision structural elucidations and verification of the magnetic anisotropy of these compounds. Studies of single crystals of the $Ba_8CoRh_6O_{21}$ oxide have shown [56] that its structure is built up of six successive RhO_6 polyhedra and a distorted CoO_6 trigonal prism. The cobalt – oxygen (2.184 – 2.197 Å) and rhodium – oxygen (1.905 – 2.055 Å) distances lie in the typical range of distances formed by these cations in similar oxides. According to calculations of the valence force sums, the Rh and Co ions in the chain are in the tetra- and divalent states, respectively, although the combination $Co^{3+} - Rh^{3+} - 5\,Rh^{4+}$ also cannot be ruled out. With this respect, it has to be noted that the valence state combination $(A')^{2+} - Rh^{4+}$ has been postulated for $Ca_3A'RhO_6$ (A = Co and Fe) based on analysis of the structural and magnetic data.[49]

IV. Low-dimensional d and p element oxides

Quasi-one-dimensional complex oxides of the family $A_{3n+3m}A'_nB_{3m+n}O_{9m+6n}$ with 3d elements occupying the B sites include cobalt and nickel compounds with the common formulas $Ca_3Co_2O_6$ ($m = 0$, $n = 1$),[60] $Sr_4Ni_3O_9$ ($m = 1$, $n = 3$),[61,62] $Ba_6Ni_5O_{15}$ (Ref. 63) and $Sr_6Co_5O_{16}$ ($m = 1$, $n = 1$);[64] manganese compounds with the formulas $Ca_3A'MnO_6$ and $Ba_6A'Mn_4O_{15}$ (A′ = Zn, Co, Cu) [65–72] and some other examples, are listed in Table 2.

Table 2. The chemical compositions of oxides of the $A_{3n+3m}A'_nB_{3m+n}O_{9m+6n}$ family (B = Co, Ni, Mn and other 3d or p elements).

m	*n*	Formula		Compound	Ref.
		gross	*x* in $A_{1+x}A'_xB_{1-x}O_3$		
1	0	ABO_3	0	$BaMnO_3$	15, 16
0	1	$A_3A'BO_6$	0.5	$Ca_3Co_2O_6$	60
				Ca_3NiMnO_6	65, 67–70
				Ca_3ZnMnO_6	65, 67, 70
				Ca_3CoMnO_6	71
				Ca_3CuMnO_6	65, 71, 72
				Ca_3ZnCoO_3	67
				$Sr_3A'CrO_6$ (A′ = Sc, In, Lu, Yb–Ho, Y)	73
				$Sr_3A'NiO_6$ (A′ = Sc, In, Tm, Yb, Lu)	74
				Sr_3PbNiO_6	75
				Ba_3NaBO_6 (B = Nb, Ta)	76
				A_3NaSbO_6 (A = Sr, Ba), A_3LiSbO_6 (A = Ca, Sr, Ba)	77
				A_3NaBiO_6 (A = Ba, Sr), Sr_3LiBiO_6	78
1	3	$A_4A'B_2O_9$	0.333	$Sr_4Ni_3O_9$	61, 62
				$Sr_4Cr_3O_9$	79
				$(Sr_{0.5}Ca_{0.5})_4Co_3O_9$	80
				$Ca_4CuMn_2O_9$	81, 82
				$Sr_4CuMn_2O_9$	21, 22, 81–83
				$Sr_4NiMn_2O_9$	82, 84–86
				$Sr_4Ni_{3-x}Mn_xO_9$	87
				$Sr_4CoMn_2O_9$	82, 88
				$Sr_4ZnMn_2O_9$	22, 89, 90
				$Sr_4MgMn_2O_9$	89
2	3	$A_5A'B_3O_{12}$	0.25	$Sr_5Co_4O_{12}$	80
				$Ba_5PdMn_3O_{12}$	91
				$Ba_5ZnMn_3O_{12}$	90
				$(Sr_{0.75}Ba_{0.25})_5NiMn_3O_{12}$	92
1	1	$A_6A'B_4O_{15}$	0.2	$(Ba_{0.25}Sr_{0.75})_6Co_5O_{15}$	80
				$Ba_6Ni_5O_{15}$	63
				$Sr_6Co_5O_{15}$	64
				$Ba_6A'Mn_4O_{15}$ (A′ = Cu, Zn)	66
				$Ba_6A'Mn_4O_{15}$ (A′ = Ni, Mg, Pd)	91, 93
4	3	$A_7A'B_5O_{18}$	0.16667	$(Ba_{0.5}Sr_{0.5})_7Co_6O_{18}$	94
				$Ba_7A'Mn_5O_{18}$ (A′ = Pd, Mg)	91, 95
5	3	$A_8A'B_6O_{21}$	0.1429	$Ba_8Co_7O_{21}$	94
				$Ba_8MgMn_6O_{21}$	95
2	1	$A_9A'B_7O_{24}$	0.125	$Ba_9Co_8O_{24}$	94
				$Ba_9MgMn_7O_{24}$	96
1	2	$A_9A'_2B_5O_{21}$	0.2857	$Sr_9Ni_2Mn_5O_{21}$	92
				$Sr_9Co_2Mn_5O_{21}$	97, 98
7	3	$A_{10}A'B_8O_{27}$	0.1111	$Ba_{10}Co_9O_{27}$	99
3	1	$A_{12}A'B_{10}O_{33}$	0.09091	$Ba_{12}Co_{11}O_{33}$	100
5	9	$A_{14}A'_3B_8O_{33}$	0.2727	$Sr_{14}Co_{11}O_{33}$	101
				$Sr_{14}Co_3Mn_8O_{33}$	98
				$Sr_{14}Cu_3Mn_8O_{33}$	21

The structures of Co and Ni complex oxides are similar to those of the platinum metal-based compounds discussed above. Typically, octahedra and trigonal prisms forming the chains going along the *c* axis contain the same d element in different oxidation states.

In contrast to the Co and Ni compounds, quasi-one-dimensional manganese oxides were obtained only in a combination with other elements occupying the trigonal prismatic sites. Such compounds can be synthesised under normal conditions in air. The manganese atoms occupy the octahedral sites, whereas the A′ sites can be occupied by such metals as Zn, Co, Ni, Cu or Mg, as in the case of platinum metal complex oxides.

1. $A_3A'MnO_6$ oxides

Manganese-containing oxides belonging to the $A_3A'MnO_6$ family were synthesised only with calcium. Ni, Co, Zn and Cu can act as A′. Attempted syntheses of $Sr_3A'MnO_6$ (A′ = Co, Ni) oxides afforded a $Sr_3NiMnO_{6.36}$ phase, which appeared similar in terms of both stoichiometry and structure to $A_4A'Mn_2O_9$ compounds ($n = 3$, $m = 1$). A transition from the initial composition of $Sr_3NiMnO_{6.36}$ to $A_4A'B_2O_9$ has resulted [84] in a modified formula, *viz*., $Sr_4(Sr_{0.20}Ni_{1.40}Mn_{1.40})O_{8.88}$.

The crystal structure of $Ca_3A'MnO_6$ with A′ = Ni, Co or Zn was refined in the space group $R\bar{3}c$ in the hexagonal setting (the Sr_4PtO_6 structural type). A similar structure was earlier confirmed for $Ca_3Co_2O_6$.[60] In this oxide, Co^{3+} cations in the octahedral and trigonal prismatic sites adopt the low-spin (LS) and high-spin (HS) states, respectively. An investigation of the formation of $Ca_3Co_{1+x}Mn_{1-x}O_6$ solid solutions gave rise to two new isostructural oxides, Ca_3CoMnO_6 and $Ca_3Co_{1.25}Mn_{0.75}O_6$.[71] The unit cell parameters of both Ca_3CoMnO_6 and $Ca_3Co_{1.25}Mn_{0.75}O_6$ are significantly larger than those of $Ca_3Co_2O_6$ due to the larger ionic radius of manganese as compared to cobalt.

The presence of cationic combinations $(A')^{2+}-Mn^{4+}$ in the $Ca_3A'MnO_6$ oxides (A′ = Ni, Co or Zn) was suggested based on the analysis of interatomic distances and magnetic susceptibility measurements. The trigonal prismatic sites in these oxides are occupied by the Co, Ni or Zn ions. (In the case of Ca_3NiMnO_6, 8% of the Mn atoms are substituted with Ni;[69,70] this explains the presence of admixturing nickel oxide NiO in the samples studied.)

The Co–O (2.140 Å) and Ni–O (2.137 Å) interatomic distances, as determined in structural studies of these phases, are close to typical values observed in other oxides with the respective metals in the divalent state. The A′–Mn interatomic distances in the chains are 2.645 Å, 2.650 Å and 2.658 Å for Co, Ni and Zn phases, respectively. So short A′–Mn distances are explained by the fact that the octahedra containing the Mn^{4+} cations are combined with the trigonal prisms with the $(A')^{2+}$ cations into the infinite chains by face-sharing. Despite the presence of short Mn–A′ contacts, no direct metal–metal bonds are formed, and all these oxides are insulators, according to the measurements of their specific resistivity.

In contrast to the manganese-based $Ca_3A'MnO_6$ oxides with A′ = Ni, Co or Zn discussed above, the crystal structure of a Ca_3CuMnO_6 oxide was refined in the triclinic space group $P\bar{1}$. According to the combined structure refinement against neutron and X-ray diffraction data, this triclinic unit cell can be derived from a *C*-centred monoclinic cell of Sr_3CuPtO_6 (the $C2/c$ space group). Nevertheless, in contrast to the structure of Sr_3CuPtO_6, there are two independent positions of both Cu and Mn atoms in the unit cell of Ca_3CuMnO_6. According to the refinement of partial occupancies of these atomic positions, 90% of the Cu(1) sites are occupied by the copper atoms, whereas 10% of them are occupied by the manganese atoms. The Cu(2) sites are exclusively occupied by copper. Both types of copper atoms are in the trigonal prismatic cavities. However, detailed analysis of the copper–oxygen interatomic distances has revealed that the coordination numbers of both types of copper atoms are better described as (4 + 2). Assuming the planar square coordination environment (the coordination number of 4), the mean copper–oxygen distances are 2.122 Å and 2.026 Å for the Cu(1) and Cu(2) sites, respectively.

Such a coordination environment is a manifestation of the Jahn–Teller effect typical of the divalent copper cations. Due to the substitution of 10% of the copper atoms in the Cu(1) sites with Mn, the mean cation–anion distances increase (2.122 Å for the coordination number of 4) and the atoms shift towards the centre of the trigonal prism. Taking into account two more remote oxygen atoms (*i.e*., for the coordination number of 4 + 2), the mean Cu(1)–O distance is 2.201 Å. Meanwhile, the Cu(2) atoms are located virtually in the centre of a lateral face of the trigonal prism. Two types of manganese atoms [*i.e*., Mn(1) and Mn(2)] are located inside the octahedra and the mean manganese–oxygen distances are 1.929 Å and 1.904 Å, respectively. A unit cell of Ca_3CuMnO_6 contains six crystallogarphically independent types of the calcium atoms, which occupy distorted square antiprismatic sites (the coordination number of 8). The mean Ca–O distances lie in the range from 2.425 Å to 2.513 Å. The octahedra accommodating the Mn(1) and Mn(2) atoms are combined with the trigonal prisms with the Cu(1) and Cu(2) atoms through face-sharing (Fig. 7) to form isolated zigzag chains composed of alternating copper and manganese atoms in a sequence: ... Mn(1)Cu(1)–Mn(2)Cu(2)Mn(1) ..., *etc*. The chains are isolated from each other with columns of distorted square antiprisms of oxygen atoms accommodating the calcium ions.

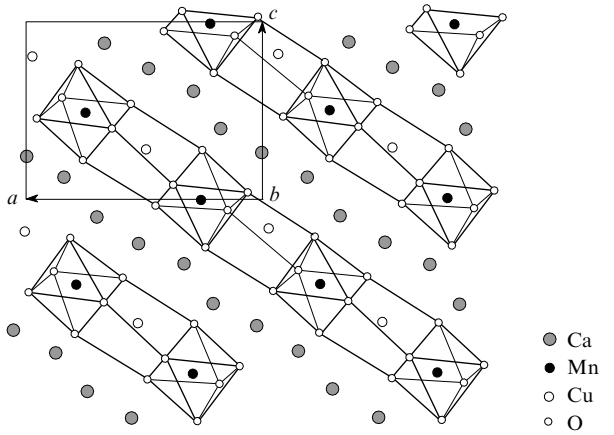


Figure 7. A projection of the crystal structure of Ca_3CuMnO_6 to the (010) plane.
A unit cell and isolated chains of the MnO_6 octahedra (two types) and CuO_6 trigonal prisms (two types) are shown.

It is of note that a minor modification of the Ca_3CuMnO_6 oxide afforded another compound, $Ca_{3.1}Cu_{0.9}MnO_6$.[102] Its crystal structure at 302 K was refined in the rhombohedral space group $R\bar{3}c$, as for other $Ca_3A'MnO_6$ (A′ = Co, Ni, Zn) oxides. However a new triclinic phase appears in the sample in addition to the rhombohedral one upon cooling to 294 K, which further becomes the dominant phase at 288 K. Similar phase transitions occurring at different temperatures were also detected for other compounds containing the Jahn–Teller Cu^{2+} ions in the A′ sites, such as $Sr_3Cu_{1-x}M_xIrO_6$ (M = Ni, Zn; $0 \leqslant x \leqslant 0.5$) and $Ca_{3.1}Cu_{0.9}RuO_6$.[102] In particular, a disordered rhombohedral structure of $Ca_{3.1}Cu_{0.9}RuO_6$ converts into an ordered monoclinic phase upon cooling to below 623 K.

2. Oxides with other stoichiometries

Some more complex oxides belonging to the family $A_{3n+3m}A'_nMn_{3m+n}O_{9m+6n}$ (with larger *n* and *m* and with a higher fraction of the octahedral sites in the chains) are also given in Table 2. Due to the similarity of ionic radii of manganese and other 3d elements, these phases possess specific structures and

manifest particular magnetic properties thus attracting a lot of attention from researchers. In particular, Melkorezova and Bazuev [87] demonstrated the existence of solid solutions with the common stoichiometry $Sr_4Ni_{3-x}Mn_xO_9$ in addition to the individual $Sr_4NiMn_2O_9$ oxide. These solid solutions were synthesised by the citrate method, which usually affords commensurate phases. However it was found that $Sr_4Ni_3O_9$ samples prepared in this way contained some amounts of NiO and SrO. The solid solutions $Sr_4Ni_{3-x}Mn_xO_9$ reveal a complex pattern of changes in the unit cell parameters (Fig. 8). The *a* parameter linearly increases with an increase in the Mn content, whereas *c* first decreases but then starts to increase passing a minimum at $x = 1.5$. The unit cell volume increases non-monotonically with an increase in *x* (*viz*., with an inflexion at $x = 1.5$). Two oppositely directed factors affect the value of *c* as a function of the solid solution composition. The first factor is a gradual replacement of smaller Ni^{4+} cations with larger Mn^{4+} cations in the B sites. The second factor is a shortening of the Ni—Mn interatomic distances due to a shift of a part of the Ni^{2+} cations in the A′ sites towards the faces of trigonal prisms. The experimental dependence of *c* on the composition indicates that the effects of the shift of Ni from the centres of prisms towards their faces prevail in the intial stages of the formation of the solid solutions (below $x = 1.5$), whereas the effects of manganese substitution for nickel starts to dominate in the late stages ($x > 1.5$).

Quarez *et al*. [103] reported the synthesis of a new representative of the $A_{3n+3m}A'_nB_{3m+n}O_{9m+6n}$ family, $Ba_4NaMn_2O_9$ ($n = 3$, $m = 1$), which is characterised by a quasi-one-dimensional structure with $a = 10.006(2)$ Å and $c = 8.210(3)$ Å (the *P*321 space group). This compound was prepared as single crystals electrochemically in NaOH melt. All attempts at the solid-state synthesis of this phase under various experimental conditions failed. In the $Ba_4NaMn_2O_9$ oxide, the sodium and manganese cations occupy the trigonal prismatic and octahedral sites, respectively. The authors argue that this compound represents the first example of manganese in the mean oxidation state of 4.5+. It has to be noted, however, that the mixed-valence state of manganese in this compound was confirmed through neither magnetic nor spectroscopic measurements. No experimental evidence on an ordered arrangement of the Mn^{4+} and Mn^{5+} ions in the available crystallographic sites was given.

A similar hexagonal phase was also detected in the Sr—Li—Mn—O system. It was synthesised by the solid-state method from manganese oxide and lithium and strontium carbonates.[104] The X-ray diffraction pattern of this phase was satisfactory indexed in the *P*321 space group with $a = 9.42(1)$ Å and $c = 7.85(1)$ Å, similarly to the respective diffraction patterns of $Sr_4Ni_3O_9$ (Ref. 61) and $Sr_{12}Ni_{7.5}O_{27}$.[105] However this phase cannot exactly correspond to the composition of $Sr_4LiMn_2O_9$, since a $Sr_7Mn_4O_{15}$ impurity is always formed in addition to the hexagonal product when the exact stoichiometric load is taken for the solid-state synthesis.[106]

A few strontium-based incommensurate oxides, *viz*., $Sr_{14}A'_3Mn_8O_{33}$ [A′ = Cu (Ref. 21) or Co (Ref. 98)] and $Sr_9A'_2Mn_5O_{21}$ [A = Ni (Ref. 92) or Co (Refs 97 and 98)], have been synthesised, whereas no Ca- or Ba-containing analogues have been reported. The idealised crystal structures of $Sr_{14}Co_3Mn_8O_{33}$ and $Sr_9Co_2Mn_5O_{21}$ are shown in Fig. 9.

Apart from Mn, Co and Ni, some other 3d transition metals form quasi-one-dimensional oxides. In particular, syntheses of chromium-containing oxides with the composition Sr_3MCrO_6 (M = Sc, In, Lu–Ho, Y) in sealed quartz ampules at 1050 °C were reported.[73] The Cr^{3+} cations in these compounds occupy the octahedral sites, whereas the trigonal prismatic sites are occupied by rare-earth elements. Probably, the $Sr_4Cr_3O_9$ oxide with a chain-like structure synthesised as single crystals (the $C_3^1-P_3$ space group, $z = 3$) [79] also belongs to this family. In this structure, the Cr^{3+} and Cr^{4+} cations occupy the octahedral and trigonal prismatic sites, respectively. A series of quasi-one-dimensional Sr_3LnNiO_6 oxides (Ln = Sc, In, Lu–Er) have been reported.[74] In these phases, the Ln^{3+} cations in the stable oxidation state stabilise nickel in the oxidation state 3+. Colourless crystals of Ba_3NaBO_6 (B = Nb, Ta) with a trigonal structure have been synthesised by Wehrum and Hoppe.[76]

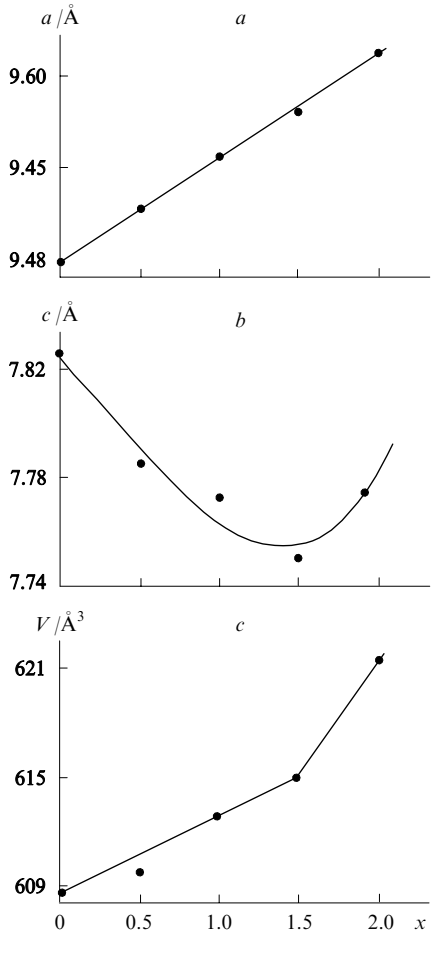


Figure 8. The unit cell parameters *a* (*a*), *c* (*b*) and volume *V* (*c*) for $Sr_4Ni_{3-x}Mn_xO_9$ solid solutions as a function of composition (*x*).

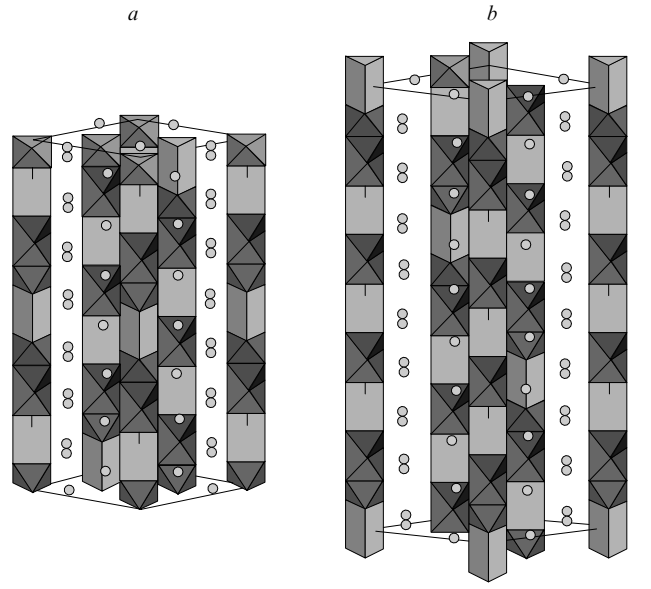


Figure 9. A polyhedral representation of the idealised crystal structures of $Sr_{14}Co_3Mn_8O_{33}$ (*a*) and $Sr_9Co_2Mn_5O_{21}$ (*b*).[98]

Some low-dimensional $A_3A'BO_6$ oxides containing p elements, in particular, Pb (Ref. 75), Sb (Ref. 77) and Bi (Ref. 78) were synthesised (see Table 2). In these oxides, antimony and bismuth have an oxidation state of +5 and occupy the octahedral B sites in the chains. In contrast, the Pb^{4+} ions occupy the trigonal prismatic sites in the Sr_3PbNiO_6 oxide.

V. Specific features of the formation of $A_{3n+3m}A'_nB_{3m+n}O_{9m+6n}$ oxides

Oxides with the stoichiometry $A_3A'BO_6$ constitute the most numerous group of compounds within the family. The A sites in the oxides of this group are occupied by divalent alkaline-earth metals, *i.e.*, Ca, Sr or Ba (among them, strontium compounds are most widespread). The cationic pairs A′B can correspond to various combinations of the oxidation states, *i.e.*, $(A')^{+}-B^{5+}$, $(A')^{2+}-B^{4+}$, $(A')^{3+}-B^{3+}$ and $(A')^{4+}-B^{2+}$ (see §). In an analysis of reasons governing the distribution of cations over the two available sites it should be taken into account that the trigonal prismatic A′ sites are characterised by a significantly larger size than the octahedral B sites. The B cations tend to occupy the octahedral sites since they typically have a higher charge and, respectively, a smaller ionic radius in the A′B pair. The Sr_3LiBiO_6 oxide represents an exception to this rule, since it is the Li^+ cations that occupy the octahedral sites in this compound.¶ The authors suggested [78] that the trigonal prismatic sites are too large to accommodate the Li^+ cations. It is of note that this oxide is crystallised in a triclinic lattice, unlike the vast majority of the $A_3A'BO_6$ compounds.

Sr_3PbNiO_6 is another exception to the above rule. In this oxide, the highly charged Pb^{4+} ions ($r = 0.775$ Å) occupy the trigonal prismatic sites, whereas the smaller Ni^{2+} cations ($r = 0.69$ Å) appear in the octahedral B sites. Smith *et al.*,[75] who synthesised the Sr_3PbNiO_6 phase for the first time, utilised the term 'inverse' to describe its structure by analogy with the normal and inverse spinels. The presence of the Ni^{2+} ions in the octahedral sites of the Sr_3PbNiO_6 oxides is very surprising since nickel occupies the trigonal pristmatic sites in all other known $A_3A'BO_6$ oxides.

The presence of large Ba^{2+} cations ($r = 1.42$ Å for the coordination number of 8) [107] in the A sites of $A_3A'BO_6$ oxides conforms to the general trend that only large alkali metal cations occupy the A′ sites in the $Ba_3A'BO_6$ oxides, where A′ = Li, Na; B = Ir, Ru, Sb, Bi, Nb, Ta). It might be suggested that a Ba_3MnBO_6 oxide containing the Mn^{2+} ions with the largest ionic radius among divalent 3d elements should exist. However this can be realised only with large tetravalent cations as B. The existence of complex oxides with the common formula A_4PtO_6 (A = Ca, Sr, Ba) with the A^{2+} cations in the trigonal prismatic A′ sites, which are characterised by similar structures, probably means that there is no limitation on the maximum radius of an A′ cation for the cationic pair $(A')^{2+}-B^{4+}$.

It has to be noted that only Ca^{2+} ions ($r = 1.12$ Å), which have the smallest ionic radius in the series $Ca^{2+}-Sr^{2+}-Ba^{2+}$, are capable of forming $A_3A'MnO_6$ oxides with the small Mn^{4+} ions in the B sites.

The influence of the size factor on the stability of the oxides has been analysed in detail for the cationic pair $(A')^{3+}-B^{3+}$. In a series of compounds with the common formula Sr_3LnRhO_6 [$r(Rh^{3+}) = 0.665$ Å], only phases with Ln = Sc, In, Yb–Sm appear stable.[51,52] For the Sr_3LnCrO_6 series [$r(Cr^{3+}) = 0.615$ Å], stable compounds were obtained with Ln = Sc, In, Lu–Ho and Y.[73] Among Sr_3LnNiO_6 oxides (the ionic radius of the Ni^{3+} cation in the low-spin state is 0.56 Å), the phases with Ln = Sc, In, Lu–Er and Y are stable.[74] It is evident that the size of the trigonal prismatic cavities is insufficient to accommodate rare-earth metal cations larger than Ho^{3+} and Y^{3+} in the latter case. The above example demonstrates that a contraction of the octahedral site due to the introduction of smaller ions instead of larger ones results in the respective contraction of the trigonal prismatic sites and *vice versa*. Exactly due to this reason, the trigonal prismatic cavity appears quite appropriate for the Li^+ cations in Sr_3LiSbO_6 but too loose in Sr_3LiBiO_6. The ionic radii of the alkaline-earth metal cations in the A (see above) and A′ sites produce analogous effects. In particular, the Mg^{2+} cation can be introduced in an A_3MgBO_6 oxide only provided that A = Sr (with the exception of Ca_3MgIrO_6).[41]

Let us now consider the specific features of the formation of the $A_{3n+3m}A'_nMn_{3m+n}O_{9m+6n}$ oxides and the influence exerted on this process by the size of cations. Manganese-containing oxides with the stoichiometry $A_3A'MnO_6$ exist only for A = Ca. Meanwhile, stable $A_4A'Mn_2O_9$ oxides are known only for Sr (with the single exception of $Ca_4CuMn_2O_9$). Barium forms groups of oxides belonging to the family starting from the composition $A_5A'Mn_3O_{12}$. As has been discussed above, the n/m ratio determines the ratio between the numbers of the $[A_3A'O_6]$ and $[A_3O_9]$ layers stacked along the c axis. In the $A_3A'MnO_6$ oxides ($n = 1$, $m = 0$), all the $[A_3O_9]$ layers are replaced with $[A_3A'O_6]$. In the $A_4A'Mn_2O_9$ oxides, three $[A_3A'O_6]$ layers occur per $[A_3O_9]$ layer. Therefore, the distance between neighbouring A_3O_9 layers should increase with an increase in the number of octahedra in the chains; this is achieved by an increase in the ionic radius of the A^{2+} cation upon the replacement of Ca with Sr and Ba. In other words, a higher fraction of octahedra in the chains requires a larger cation in the A site.

The cationic compositions of the $A_3A'BO_6$ oxides is similar to the compounds from the Ruddlesden–Popper family (*i.e.*, $A_3B_2O_7$ or $A_{n+1}B_nO_{3n+1}$ with $n = 2$). Taking into account that some of the Ruddlesden–Popper oxides contain two different cations in the B sites [*e.g.*, $Sr_3FeCoO_{7-\delta}$,[108] $Sr_3Fe_{2-x}Mn_xO_{7-\delta}$ (Ref. 109)] and the oxygen deficiency δ can be as large as 1, it might be expected that they undergo structural transitions into quasi-one-dimensional structures. Indeed, a transition from the Ruddlesden–Popper structure to a quasi-one-dimensional structure of the $A_3A'BO_6$ type was observed in $Sr_3ScCoO_{6+\delta}$.[110] The former phase, $Sr_3ScCoO_{6.08}$, was synthesised at 1250 °C, whereas the latter, at 1100 °C. However the quasi-one-dimensional Sr_3ScCoO_6 complex oxide undergoes amorphisation and probably decomposition upon storage in air.

VI. Magnetic properties

The presence of transition metals and the quasi-one-dimensional character determines the specific magnetic properties of the oxides under consideration. The relation of magnetic properties to the structure is governed to a large extent by a high degree of mutual isolation of the $[A'B_nO]_\infty$ chains. According to magnetic studies of single crystals of these compounds, the low-dimensional character of their structures gives rise to a pronounced anisotropy of their magnetic properties. These systems typically undergo magnetic ordering at low temperatures. Notwithstanding, some compounds from the $A_{3n+3m}A'_nB_{3m+n}O_{9m+6n}$ family are characterised by relatively high temperatures of the magnetic ordering, despite their quasi-one-dimensional structures. In particular, $Ca_3A'RuO_6$ oxides (A′ = Li, Na) manifest a collinear magnetic structure with the Neél temperature of $T_N \approx 100$ K.[9] So high value of T_N implies a three-dimensional antiferromagnetic ordering. $Sr_3A'BO_6$ complex oxides manifest the whole spectrum of magnetic properties (Table 3): they reveal either 1D-antiferromagnetism or ferromagnetism. Furthermore, ferromagnetic interactions inside the chain and antiferromagnetic interchain interactions are typical of these phases. The disordered quantum spin chain paramagnetism has been discovered for the first time in a compound from this family,

§ It is of note that strontium forms compounds with all possible cationic pairs, whereas barium-containing oxides are known mainly for the $(A')^{+}-B^{5+}$ cationic pairs.

¶ The Li^+ and Bi^{5+} cations are characterised by identical ionic radii (0.76 Å).[107]

Table 3. The magnetic properties of $Sr_3A'BO_6$ oxides (A′ = Ni, Cu, Zn, Co; B = Ir, Pt).

Compound	Properties
Sr_3NiIrO_6	antiferromagnetism
Sr_3CuIrO_6	ferromagnetism
Sr_3ZnIrO_6	antiferromagnetism
Sr_3NiPtO_6	"
Sr_3CuPtO_6	"
Sr_3CoPtO_6	disordered spin chain paramagnetism
Sr_3ZnPtO_6	diamagnetism
$Sr_3CuIr_{0.5}Pt_{0.5}O_6$	disordered spin chain paramagnetism

$Sr_3CuPt_{0.5}Ir_{0.5}O_6$ (see Ref. 8). The $Ca_3Co_2O_6$ oxide undergoes the ferrimagnetic ordering at $T < 25$ K (Ref. 111) due to the ferromagnetic and antiferromagnetic exchange interactions between the cobalt cations located within the same chain and in neighbouring chains, respectively.

For the analysis of magnetic properties it would be convenient to subdivide the $A_3A'BO_6$ compounds into two groups: in the first group, magnetic cations occupy exclusively the octahedral sites and in the second group, the magnetic cations occupy both the octahedral and trigonal prismatic sites. In the former case, the distance between magnetic cations located in different chains is only slightly larger than that within the same chain. Usually, changes in the magnetic susceptibility (χ) for such compounds are interpreted within the one-dimensional Ising model. The interactions between the magnetic cations typically give rise to the antiferromagnetic correlations with maxima in $\chi = f(T)$ curves. Normally, no long-range magnetic ordering is observed in these compounds.

On the other hand, $A_3A'BO_6$ compounds with magnetic ions occupying both the A′ and B sites often manifest a complex magnetic behaviour due to an interplay between the intrachain and interchain magnetic interactions. In particular, a magnetic structure was revealed for $Ca_3Co_2O_6$ in a low-temperature neutron diffraction study. Meanwhile, no magnetic reflections were observed in other isostructural compounds (such as Sr_3NiIrO_6).[7] Taking into account that the basal plane in the crystal structure of Sr_3NiIrO_6 is described by a 2D hexagonal lattice (*i.e.*, each chain is surrounded by six neighbouring chains), it might be assumed that the lack of the magnetic ordering is caused by either a disorder in the distribution of the transition metal atoms over the crystallographic sites or a specific geometric structure of the crystal (the geometric frustration).

The magnetic properties of $A_3A'BO_6$ oxides (B = Pt, Ir, Rh, Ru) are strongly dependent on the electronic configuration of metals occupying both the A′ and B sites. Many of these compounds are similar in terms of their structures but their magnetic properties are manifold. In the $Sr_3A'PtO_6$ oxides (A′ = Cu, Co, Ni, Zn), the platinum atoms occupying the octahedral sites are in the low-spin (diamagnetic) state. As a consequence, the Sr_3ZnPtO_6 oxide with the diamagnetic Zn^{2+} cation behaves as a diamagnetic. In contrast, according to the magnetic susceptibility measurements, the Ni^{2+} cations in the Sr_3NiPtO_6 oxide manifest a strong one-ion magnetic anisotropy, which induces the local antiferromagnetic ordering at $T < 25$ K.[32] Furthermore, Sr_3CoPtO_6 reveals the disordered spin chain paramagnetism. According to the magnetic susceptibility and heat capacity measurements, the behaviour of Sr_3CuPtO_6 (Refs 32 and 112) is well described by theoretical models for classical spin chain compounds with $S = 1/2$. It is ferromagnetism that is typical of such compounds (see Table 3).

The iridium-based $Sr_3A'IrO_6$ oxides are characterised by a more complex pattern of magnetic behaviour due to the replacement of the diamagnetic Pt^{4+} cations in the octahedral sites with the low-spin $Ir^{4+}(d^5)$ cations having an unpaired electron. The magnetic susceptibility of Sr_3ZnIrO_6 above the antiferromagnetic transition (25 K) is well described by the Heisenberg linear chain model. The magnetic properties of Sr_3NiIrO_6 evolve in a complicated manner as a function of temperature, which is due to an interplay between the ferromagnetic interchain and antiferromagnetic intrachain exchange interactions. The first preliminary conclusion[7] on the ferromagnetic behaviour of Sr_3CuIrO_6 was corrected in more recent studies. Actually,[113] below the magnetic transition temperature in the zero field, this compound behaves as a spin glass, but it converts into the ferromagnetic state already in a weak magnetic field (~200 Œ). Similarly, detailed investigations[114, 115] into the magnetic properties of $Sr_3Cu_{1-x}Zn_xIrO_6$ and $Sr_3CuPt_xIr_{1-x}O_6$ solid solutions reveal a more complex character of the magnetic interactions both in the individual quasi-one-dimensional oxides and solid solutions than that reported initially.

The Ca_3CuIrO_6 and Ca_3CuRhO_6 oxides undergo the magnetic ordering[116] at ~15 K, but the nature of these magnetic transitions is rather complex. As for Co-based oxides, Ca_3CoIrO_6 undergoes the frustrated magnetic ordering below 30 K.[38, 117] Meanwhile, the Ca_3CoRuO_6 oxide behaves as a normal antiferromagnetic with $T_N = 55$ K.[38]

When polycrystalline samples are studied, no saturation magnetisation can be achieved even in very strong magnetic fields, which is a specific feature of the magnetic properties of quasi-one-dimensional oxides. Therefore, accurate values of the saturation magnetisation and, consequently, ferromagnetic moments can only be determined for single crystals by performing careful measurements along specific crystallographic directions. The ferromagnetic moment of $Ca_3Co_2O_6$ was measured for a polycrystalline sample mixed with epoxy resin magnetised in a field of 80 kŒ.[111] As a result of this treatment, the sample had a strong preferred orientation along the *c* axis and manifested highly anisotropic magnetic properties (Fig. 10). The character of the observed dependence of magnetisation *M* on the applied magnetic field strength *H* indicates that the ferromagnetic chains ($T_{C_1} = 26$ K) interact antiferromagnetically ($T_{C_2} = 13$ K). In weak fields, this system occurs in the partially disordered antiferromagnetic (PDA) state at $10 \leqslant T \leqslant 25$ K but converts into the ferrimagnetic state at $T < 10$ K. In the PDA state, one third of the chains are magnetically disordered while two third of the chains are ferromagnetic and interact with each other antiferromagnetically.

Smith and co-workers[56] observed a strong anisotropy of the magnetic susceptibility χ of single-crystalline $Ba_8CoRh_6O_{21}$ ori-

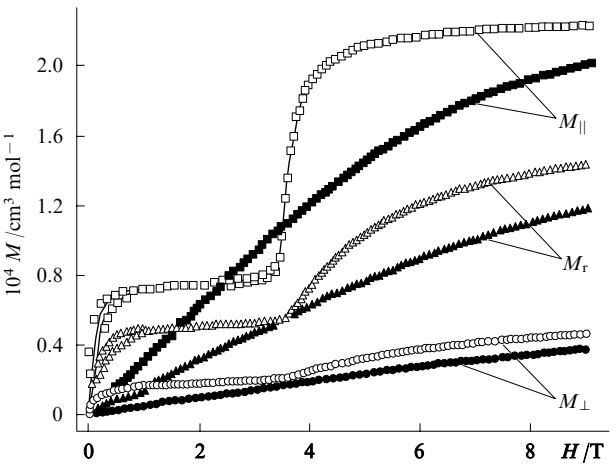


Figure 10. The magnetisation curves of $Ca_3Co_2O_6$ measured in a magnetostatic field of a strength $0 \leqslant H \leqslant 9$ T at 12 K (open symbols) and 35 K (closed symbols).[111]
$M_{||}$, $M_\perp$ are the magnetisation values measured for the sample oriented with its *c* axis parallel and perpendicular to the applied magnetic field, respectively; M_r is the magnetisation for an unoriented samples.

ented with the crystallographic c axis either parallel or perpendicular to the applied magnetic field. The anisotropy is preserved up to room temperature. The rhodium cations in the $A_3A'RhO_6$ oxides can be tri-, tetra- or pentavalent, depending on the oxidation state of an element in the A′ sites. The magnetic properties of the Sr_3LnRhO_6 compounds were interpreted [52] assuming expected values of the magnetic moments for the Ln^{3+} cations and the low-spin state for the Rh^{3+} cations ($t_{2g}^6e_g^0$, $S = 0$). The cobalt and iron cations in Ca_3CoRhO_6 and Ca_3FeRhO_6 are divalent, while rhodium is tetravalent, according to measurements of χ.[49] Presumably, the temperature dependence of the magnetic properties of Ca_3CoRhO_6 is similar to that of Sr_3NiIrO_6 and Ca_3CoIrO_6. The magnetic susceptibility measured in the zero-field cooling (ZFC) mode drops down at 35 K, whereas it remains virtually constant upon cooling in a magnetic field (*i.e.*, in the FC mode). According to the results reported by Niitaka *et al.*,[49] this compound is characterised by the antiferromagnetic interchain exchange interactions coupled with the ferromagnetic intrachain interactions. Neutron diffraction studies [118] showed that this compound occurs at $T < 90$ K in the partially disordered antiferromagnetic state (1/3 of the chains are magnetically disordered, while 2/3 of the chains are ordered ferromagnetically and interact with each other antiferromagnetically). According to recent results by Niitaka *et al.*[118] (in contrast to earlier data [49] on the magnetic susceptibility), both transition metals in the Ca_3CoRhO_6 oxide are trivalent. This conclusion is supported by an analysis of the oxidation states of cations in $Ca_3Co_2O_6$ and Ca_3CoRhO_6 based on theoretical electron band structure calculations.[119] Despite the pronounced similarity between these two compounds in terms of both their structures and magnetic properties, the antiferromagnetic interchain interactions therein are substantially different, as evidenced by measurements of the specific heat capacity.[120] Studies of related rhodium oxides with the Co atoms substituted with Fe and Zn revealed that the Ca_3FeRhO_6 oxide undergoes a three-dimensional antiferromagnetic transition at 12 K, while Sr_3ZnRhO_6 experiences an inhomogeneous magnetic ordering below $\sim$15 K.[121] The antiferromagnetic interactions at $T < 10$ K were also observed [122] for Sr_4RhO_6 and Sr_3CaRhO_6. Mwamuka *et al.*[123] elucidated the magnetic behaviour of $Sr_4Fe_{0.73}Rh_{2.27}O_9$. Unfortunately, the experimental data on χ obtained were insufficient to unambiguously establish the oxidations states of Fe and Rh in this compound. A maximum in the $\chi = f(T)$ curve at 8 K points to a probable antiferromagnetic ordering.

Manganese-based complex oxides also exhibit diverse magnetic properties. The antigerromagnetic ordering in Ca_3ZnMnO_6 and Ca_3NiMnO_6 was established by means of neutron diffraction.[67] It is of note that that the Ca_3ZnMnO_6 oxide, where a half of cationic positions in the chains (*viz.*, trigonal prismatic sites) are occupied by the diamagnetic Zn^{2+} ions, is characterised by a significantly lower Neél temperature ($T_N = 25$ K) than $Ca_3A'RuO_6$ (A′ = Li, Na). The Ca_3NiMnO_6 oxide containing magnetic cations in both the octahedral and trigonal prismatic sites is an antiferromagnetic with $T_N = 20$ K (according to Ref. 67) or 18 K (according to Ref. 69). The $\chi = f(T)$ curve for this oxide obeys the Curie–Weiss law only above 300 K, which is probably due to the preservation of the local magnetic ordering up to high temperatures. In contrast to the ferro(ferri)magnetic $Ca_3Co_2O_6$ compound, its Mn-analogue, Ca_3CoMnO_6, reveals the long-range antiferromagnetic ordering ($T_N = 13$ K).[71, 124] It has to be however noted that only short-range magnetic ordering was revealed in Ca_3CoMnO_6 at 4.2 K using neutron diffraction:[71] only broad weak reflexes were observed in the diffraction pattern instead of distinct magnetic reflections. Furthermore, the heat capacity *vs.* temperature curve for this phase has a kink at 13 K, which is indicative of magnetic correlations extending to a part of the crystal rather than to the whole crystal.[124] Probably, this is a reason for the absence of magnetic reflections in the neutron powder diffraction pattern of this compound. The magnetic properties of $Ca_3Co_{1.25}Mn_{0.75}O_6$ are similar to those of Ca_3CoMnO_6 except for a higher T_N (18 K). For these phases, both the ferromagnetic ordering and spin glass state can be decisively ruled out. These oxides undergo spin-reorientation transitions at $T \leqslant 5$ K, as evidenced by the hysteresis loops in their magnetisation curves.

According to the measurements of the magnetic susceptibility and heat capacity,[71, 125] the triclinic Ca_3CuMnO_6 oxide undergoes the antiferromagnetic ordering at $T < 6$ K. This compound manifests strict long-range magnetic order and is not liable to the magnetic structure frustration, despite the positional disorder of the Cu^{2+} and Mn^{4+} cations and the presence of several types of these cations, which are characterised by different Cu–O and Mn–O bond lengths. The heat capacity *vs.* temperature curve reveals two distinct λ-peaks at 5.2 K and 3.6 K. The experimental data [69–72] on the magnetic susceptibility of $Ca_3A'MnO_6$ are shown in Fig. 11.

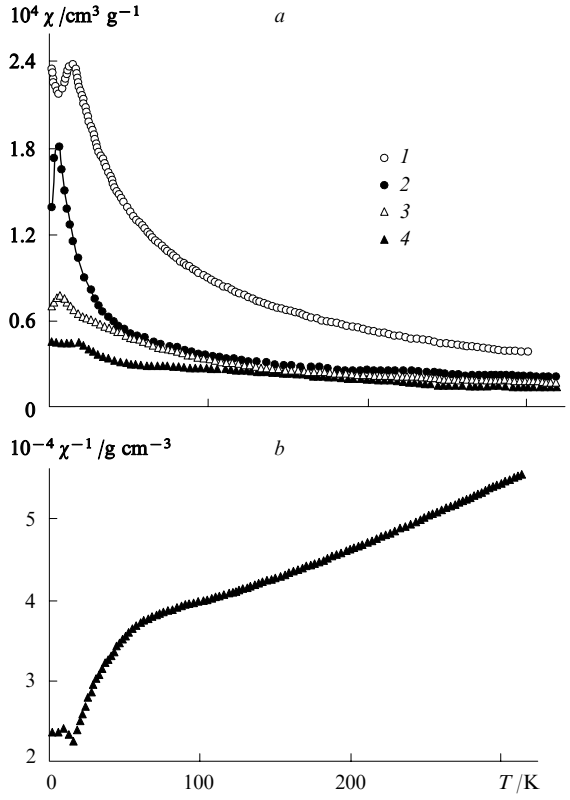


Figure 11. The temperature dependences of magnetic susceptibility (*a*) and the Curie–Weiss plots (*b*) for a series of $Ca_3A'MnO_6$ oxides. A′ = Co (*1*), Cu (*2*), Zn (*3*), Ni (*4*).

The magnetic susceptibility of $Sr_4ZnMn_2O_9$ and $Sr_4MgMn_2O_9$ as a function of temperature is shown in Fig. 12.[89] It is clearly seen that the magnetic susceptibility of these oxides reveals a complex temperature dependence at $T < 250$ K and does not obey the Curie–Weiss law. The apparent magnetic moments approach the purely spin value of the Mn^{4+} ions at a high temperature. The $\chi(T)$ curves exhibit a broad maximum at 100–150 K, which is more pronounced in the case of $Sr_4ZnMn_2O_9$. These experimental data on $\chi(T)$ for $Sr_4ZnMn_2O_9$ and $Sr_4MgMn_2O_9$ were analysed within a model of the isotropic exchange interactions between the Mn^{4+}–Mn^{4+} dimers. The dramatic increase in the magnetic susceptibility at low temperature obeys the Curie–Weiss law, which indicates that not all the Mn^{4+} ions in $Sr_4ZnMn_2O_9$ and $Sr_4MgMn_2O_9$ are combined into dimers.

Similar conclusions were derived for $Sr_4NiMn_2O_9$ (Refs 84–86) and $Sr_4CuMn_2O_9$ (Refs 20, 22 and 81). Each

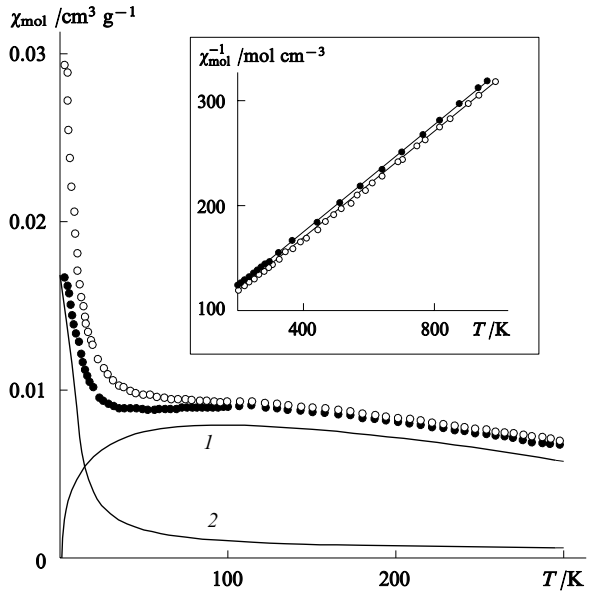


Figure 12. The temperature dependences of magnetic susceptibility for $Sr_4MgMn_2O_9$ (open circles) and $Sr_4ZnMn_2O_9$ (closed circles).[84]
The curves *1* and *2* show the contributions of the dimeric and paramagnetic components. The Curie–Weiss plot for the compound showing the linearity in the temperature range of 300–950 K is given in the inset.

Mn^{4+} ion in the chains present in the crystal structures of the $A_4A'Mn_2O_9$ oxides is involved in the exchange interactions with a neighbouring Mn^{4+} cation and a divalent cation (Zn, Mg, Ni or Cu). It is the exchange interactions between the Mn^{4+} ions that dominate the magnetic susceptibility of these phases at $T < 250$ K, although nickel and copper have their own unpaired electrons in the d shells (in contrast to zinc and magnesium). The contribution from the exchange interactions between the Mn^{4+} and Ni^{2+} (Cu^{2+}) ions is negligibly small.

Among the $A_4A'Mn_2O_9$ oxides, $Sr_4CoMn_2O_9$ is worthy of a special note. The temperature dependence of inversed magnetic susceptibility for this compound at $T > 150$ K obeys the Curie–Weiss law[82]

$$\chi = \frac{C}{T - \Theta}.$$

The paramagnetic moment experimentally measured in this temperature range (6.61 μ_B) is close to the theoretical value calculated for the cationic combination $Co^{2+} - 2\,Mn^{4+}$ (6.71 μ_B). The negative value of Θ (−120 K) indicates that the antiferromagnetic interactions dominate. This oxide exhibits a spontaneous magnetisation at $T < 12$ K. In order to analyse the origin of this low-temperature magnetism, real and imaginary parts of the dynamical magnetic susceptibility were measured in the frequency range from 0.1 Hz to 10 kHz. It was found that the $Sr_4CoMn_2O_9$ oxide is characterised by a partially disordered magnetic structure close to that typical of spin glasses and different from that of $Sr_4NiMn_2O_9$, where pairs of the Mn^{4+} ions interact antiferromagnetically along the chains. Similar magnetic properties were observed in $Sr_{14}Co_3Mn_8O_{33}$ (Ref. 98) and $Sr_9Co_2Mn_5O_{21}$ (Refs 97 and 98). The temperature dependence of the magnetic susceptibility plotted in the coordinates $1/\chi = f(T)$ for some of the $A_4A'Mn_2O_9$ oxides discussed above are shown in Fig. 13. A step observed for $Ca_4CuMn_2O_9$ at 123 K is attributed to the presence of the perovskite $CaMnO_3$ phase, manifesting a weak ferromagnetism at $T < 123$ K, in the sample studied.

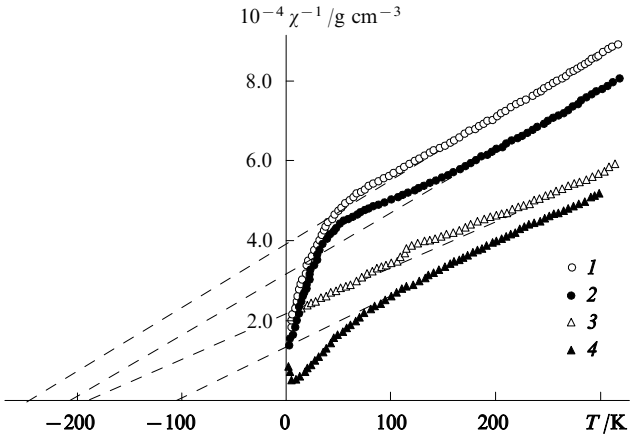


Figure 13. The Curie–Weiss plots for $Sr_4NiMn_2O_9$ (*1*), $Sr_4CuMn_2O_9$ (*2*), $Ca_4CuMn_2O_9$ (*3*) and $Sr_4CoMn_2O_9$ (*4*).[82]

In the case of $Ba_6ZnMn_4O_{15}$, the magnetic suscpetibility as a function of temperature deviates from the Curie–Weiss law in a temperature range of 4.2–300 K,[66] which is manifested in a drastic increase in χ at $T < 16$ K and a broad local maximum in the $\chi = f(T)$ curve at 45 K. It was suggested that the short-range antiferromagnetic interactions between the Mn^{4+} cations giving rise to the one-dimensional alignment of magnetic moments in the face-sharing octahedra is preserved up to 300 K. The increase in χ at $T < 16$ K is due to the contribution of the Mn^{4+} cations with uncompensated (owing to the structual disorder) magnetic moments into the total magnetic susceptibility.

The temperature dependence of the magnetic susceptibility for $Ba_6CuMn_4O_{15}$ was interpreted[66] as a joint effect of the paramagnetism of the Cu^{2+} ions in the trigonal prismatic sites and the ordering of the Mn^{4+} cations (that gives rise to a broad maximum at 90 K). The neutron diffraction patterns of $Ba_6CuMn_4O_{15}$ and $Ba_6ZnMn_4O_{15}$ measured at 1.7 K revealed magnetic reflections attributable to the appearance of the long-range magnetic order of the ions in the octahedral sites. The magnetic behaviour of these oxides was simulated using an unusual magnetic structure, in which the antiferromagnetic superexchange interactions in a strongly frustrated crystal structure gives rise to a rotation of spins in neighbouring chains by 120°.

The magnetic properties of the $Ba_6A'Mn_4O_{15}$ oxides (A′ = Mg, Ni)[94] differ significantly from those of their zinc and copper analogues.[66] In particular, the $\chi = f(T)$ curve for the $Ba_6MgMn_4O_{15}$ oxide reveals no broad maxima at intermediate temperatures. This compound follows the Curie–Weiss law at $T > 125$ K. Since the magnetic susceptibilities of $Ba_6ZnMn_4O_{15}$ and $Ba_6MgMn_4O_{15}$ are governed exclusively by the exchange interactions between the Mn^{4+} cations, the differences between these two phases should be attributed to different distributions of the Mn^{4+} cations over the octahedral and trigonal prismatic sites therein. The experimentally determined value of the Curie constant for $Ba_6NiMn_4O_{15}$ appeared smaller than the respective theoretical value calculated as a joint contribution from the nickel and manganese cations. This discrepancy can be explained assuming that a part of the Ni^{2+} cations adopt the planar square coordination. This fraction should amount to ~28% to reconcile the experimental and theoretical values of the Curie constant.

The experimental data on the magnetic susceptibility and magnetisation of $Ba_9MgMn_7O_{24}$ (Ref. 96) are close to the respective results for $Ba_5PdMn_3O_{12}$, $Ba_6PdMn_4O_{15}$ and $Ba_7PdMn_5O_{18}$.[91] In particular, a deviation of the $1/\chi = f(T)$ curve from the Curie–Weiss law is observed at $T < 225$ K owing to the magnetic ordering of the Mn^{4+} cations in the quasi-one-dimensional chains $-MgO_6-(MnO_6)_7-MgO_6-(MnO_6)_7-$ composed of trigonal prisms accommodating the Mg^{2+} cations and octahedra occupied by Mn^{4+}. Additionally, a

specific character of the magnetic susceptibility as a function of the applied magnetic field strength at 2 K suggests a low ferromagnetic moment.

It would be interesting to compare the magnetic properties of oxides from the $A_{3n+3m}A'_nMn_{3m+n}O_{9m+6n}$ family with those of $BaMnO_3$, the ultimate representative of the family.[16] The magnetic susceptibility of $BaMnO_3$ and many quasi-one-dimensional oxides of the family deviates from the Curie–Weiss law in a temperature range from 4.2 K to 300 K. Furthermore, at temperatures $T < 215$ K, the magnetic susceptibilities χ measured in a magnetic field and in the zero field are different; the reason for this discrepancy remains unclear. The transition from a paramagnetic into a magnetically ordered state occurs at 59 K. Probably, this transition for $BaMnO_3$ and other $A_{3n+3m}A'_nMn_{3m+n}O_{9m+6n}$ oxides differs from ordinary transitions from a paramagnetic into an antiferromagnetic state. It should rather be considered as a transition from a 1D-magnetically ordered state into a 3D-ordered one. Within the chains, the spins of neighbouring Mn^{4+} cations interact antiferromagnetically and lie in the plane perpendicular to [001]. The comparative analysis of the magnetic properties of $BaMnO_3$ and other known $A_{3n+3m}A'_nMn_{3m+n}O_{9m+6n}$ oxides with $A' = Zn^{2+}$, Mg^{2+} demonstrates their essential similarity. This implies that in the case of compounds with diamagnetic cations in the trigonal prismatic sites, the interchain magnetic exchange prevails over the intrachain interactions. But when a second magnetic cation is introduced into the $[A'Mn_nO]_\infty$ chains, the pattern of magnetic behaviour becomes more complex. Jordan *et al.*[98] pointed out that the magnetic properties of the quasi-one-dimensional phases, such as $Sr_3NiRhO_{6+\delta}$, $Sr_3CuRhO_{6+\delta}$, $Sr_4NiMn_2O_9$ and $Ca_3Co_{1+x}Mn_{1-x}O_6$, are extremely sensitive to the positional disorder within the chains and structural transitions.

Interesting results were obtained in a study of $Ca_3A'MnO_6$ ($A' = Zn$, Cu, Ni, Co), solid solutions $Ca_3Zn_{1-x}Cu_xMnO_6$ ($0 \leqslant x < 0.75$) isostructural to the hexagonal K_4CdCl_6 phase, $Ca_3Zn_{0.25}Cu_{0.75}MnO_6$ (with a triclinic lattice similar to that of Ca_3CuMnO_6) and $Ca_4A'Mn_2O_9$ by means of ESR.[126, 127] The ESR spectra of the $Ca_3A'MnO_6$ oxides ($A' = Zn$, Cu) revealed intense signals of the Mn^{4+} cations, although there were no features attributable to Cu^{2+}. Furthermore, the integral spectral intensity and g-factors were temperature dependent. The lack of ESR signal from the copper ions in the spectra of Ca_3CuMnO_6 and solid solutions $Ca_3Zn_{1-x}Cu_xMnO_6$ ($0 \leqslant x < 1$) can be due to the planar square coordination of the Cu ions in these compounds. A weak signal emerging in the spectrum of the quasi-one-dimensional Ca_3CuMnO_6 oxide following its annealing at 470 K can indicate[102] a change in the coordination type of the Cu^{2+} ions. Therefore, it might be suggested that the compound undergoes a structural phase transition at $T > RT$.

The ESR spectra of $Ca_3A'MnO_6$ ($A' = Ni$, Co) revealed no signals of the Mn^{4+} ions. The intensities of the observed lines (which are 4 orders of magnitude smaller than in the case of the oxides with $A' = Zn$, Cu) with $g = 2.11$ and widths $\Delta H \sim 590$ G are virtually independent of temperature in the range of 77–490 K.

According to the analysis of the ESR features of the Mn^{4+} cations in the spectrum of Ca_3CuMnO_6, a weak antiferromagnetic ordering exists already at 300 K. Taking into account the absence of ESR signals of Mn^{4+} in the spectra and the lack of the magnetic order in $Ca_3A'MnO_6$ with $A' = Ni$ or Co, it might be suggested that relatively strong exchange interactions are realised between the nickel (cobalt) and manganese cations, which give rise to a redistribution of the electron density and a change in the charge state of the A' cations from 2+ to 3+ and, respectively, of the manganese cations from 4+ to 3+, in contrast to structural data that are indicative of the cationic combinations $(A')^{2+}-Mn^{4+}$.

The ESR spectra of the $Sr_4A'Mn_2O_9$ oxides ($A' = Zn$, Cu, Ni) also reveal distinct signals of Mn^{4+} and no signals of Cu^{2+} and Ni^{2+}.

* * *

An analysis of the available information concerning quasi-one-dimensional oxides of the $A_{3n+3m}A'_nB_{3m+n}O_{9m+6n}$ family indicates that the number of theoretically predicted compounds belonging to the family presently significantly exceeds the number of actually synthesised and characterised compounds. This is equally true for platinum metal- and manganese-based complex oxides. Most probably, the major reason for this is a similar chemical composition of possible phases, which impedes the purposeful search for conditions of their synthesis. For instance, Bazuev *et al.*[81] studied the Ca–Cu–Mn–O system and obtained two compounds, Ca_3CuMnO_6 and $Ca_4CuMn_2O_9$. The latter phase contained admixtures of CuO (according to powder X-ray diffraction data) and $CaMnO_3$ (according to magnetic measurements). This compound is incommensurate. The ratio $c_1/c_2 = 0.6891$ is significantly larger than the value 0.66_6 typical of phases with this stoichiometry but rather close to the value of 0.6923 expected for a commensurate phase with the composition $A_{18}A'_5Mn_8O_{39}$ ($m = 1$, $n = 5$). Hopefully, the experimental conditions required to stabilise both these phases, *i.e.*, $Ca_4CuMn_2O_9$ and $Ca_{18}Cu_5Mn_8O_{39}$ will be found in the future.

The vast majority of quasi-one-dimensional oxides known to date have been synthesised using solid-state reactions, therefore, more efforts should be put forth for the search for conditions of solid-state syntheses affording single crystals of desired size and quality.

Although magnetic parameters are reported in virtually any study dealing with the synthesis of new oxides of the $A_{3n+3m}A'_nB_{3m+n}O_{9m+6n}$ family, the general trends in the magnetic behaviour of quasi-one-dimensional compounds have not been elucidated in sufficient details. This relates to complex correlations between the structure of these compounds (including such features as short metal–metal distances within the chains and a substantial separation of neighbouring chains), electronic configuration of the d elements in the A' and B sites and their properties. The nature of low-temperature magnetic phases has not been determined to date. The interrelations between changes in the chemical composition of the compounds at the course of their synthesis and their magnetic behaviour are yet to be established.

For the compounds containing several (most frequently, two) transition metal cations in the $[(A'B)O_3]_\infty$ chains, the determination of valency combinations $A'-B$ becomes a challenge. As follows from the above discussion, even accurate structural data are insufficient in some cases to rationalise the results of magnetic measurements. This problem is especially severe for cobalt-containing compounds. Presumably, the involvment of theoretical methods for the electron structure calculation will help to overcome this problem.

References

1. J Darriet, M A Subramanian *J. Mater. Chem.* **5** 543 (1995)
2. J M Perez-Mato, M Zakhour-Nakhl, F Weill, J Darriet *J. Mater. Chem.* **9** 2795 (1999)
3. J J Randall Jr, L Katz *Acta Crystallogr.* **12** 519 (1959)
4. G Bergerhoff, O Schmitz-Dumond *Z. Anorg. Allg. Chem.* **284** 10 (1956)
5. A P Wilkinson, A K Cheetham, W Kunnman, A Kvick *Eur. J. Solid State Inorg. Chem.* **28** 453 (1991)
6. J L Hodeau, H Y Tu, P Border, T Fournier, P Strobel, M Marezio *Acta Crystallogr., Sect. B* **48** 1 (1992)
7. T N Nguyen, H-C zur Loye *J. Solid State Chem.* **117** 300 (1995)
8. T N Nguyen, P A Lee, H-C zur Loye *Science* **271** 489 (1996)
9. J Darriet, F Grasset, P D Battle *Mater. Res. Bull.* **32** 139 (1997)
10. P D Battle, G R Blake, J Sloan, J F Vente *J. Solid State Chem.* **136** 103 (1998)
11. P D Battle, G R Blake, J Darriet, J G Gore, F Weil *J. Mater. Chem.* **7** 1559 (1997)

12. G R Blake, J Sloan, J F Vente, P D Battle *Chem. Mater.* **10** 3536 (1998)
13. K E Stitzer, J Darriet, H-C zur Loye *Curr. Opin. Solid State Mater. Sci.* **5** 535 (2001)
14. J J Lander *Acta Crystallogr.* **4** 148 (1951)
15. B L Chemberland, A W Sleight, J F Weiher *J. Solid State Chem.* **1** 506 (1970)
16. E J Cussen, P D Battle *Chem. Mater.* **12** 831 (2000)
17. A F Wells *Structural Inorgan Chemistry* (Oxford: Clarendon Press, 1977)
18. M-H Whangbo, H-J Koo, K-S Lee, O Gourdon, M Evain, S Jobic, R Brec *J. Solid State Chem.* **160** 239 (2001)
19. M Evain, F Boucher, O Gourdon, V Petricek, M Dusek, P Bezdicka *Chem. Mater.* **10** 3068 (1998)
20. R C Layland, H-C zur Loye *J. Alloys Compd.* **299** 118 (2000)
21. A El Abed, E Gaudin, H-C zur Loye, J Darriet *Solid State Sci.* **5** 59 (2003)
22. C A Moore, P D Battle *J. Solid State Chem.* **176** 88 (2003)
23. A M Abakumov, A V Mironov, V A Govorov, M V Lobanov, M G Rozova, E V Antipov, O I Lebedev, G Van Tendeloo *Solid State Sci.* **5** 1117 (2003)
24. A V Mironov, A M Abakumov, E V Antipov *Rigaky J.* **19 – 20** 23 (2003)
25. R Czaya *Z. Anorg. Allg. Chem.* **375** 61 (1970)
26. J B Claridge, R C Layland, H-C zur Loye *Acta Crystallogr., Sect. C.* **53** 1740 (1997)
27. W D Komer, D J Machin *J. Less-Common Met.* **61** 91 (1978)
28. Y H Wang, D Walker, B H Chen, B A Scott *J. Alloys Compd.* **285** 98 (1999)
29. A Varela, K Boulahya, M Parras, J M González-Calbet, T Vogt, D J Butter *Chem. – Eur. J.* **7** 1444 (2001)
30. A P Wilkinson, A K Cheetham *Acta Crystallogr., Sect. C* **45** 1672 (1989)
31. A Tomaszewska, Hk Müller-Buschbaum *Z. Anorg. Allg. Chem.* **617** 23 (1992)
32. T N Nguyen, D M Giaquinta, H-C zur Loye *Chem. Mater.* **6** 1642 (1994)
33. T N Nguyen, H-C zur Loye *MRS Symp. Proc.* **376** 603 (1995)
34. M D Smith, H-C zur Loye *Acta Crystallogr., Sect. C* **57** 337 (2001)
35. P Núñez, S Trail, H-C zur Loye *J. Solid State Chem.* **130** 35 (1997)
36. M J Davis, M D Smith, H-C zur Loye *Inorg. Chem.* **42** 6980 (2003)
37. J B Claridge, R C Layland, R D Adams, H-C zur Loye *Z. Anorg. Allg. Chem.* **623** 1131 (1997)
38. H Kageyama, K Yoshimura, K Kosuge *J. Solid State Chem.* **140** 14 (1998)
39. A Tomaszewska, Hk Müller-Buschbaum *Z. Anorg. Allg. Chem.* **619** 534 (1993)
40. J B Claridge, R C Layland, W H Henley, H-C zur Loye *Z. Anorg. Allg. Chem.* **624** 1951 (1998)
41. M J Davis, M D Smith, H-C zur Loye *Acta Crystallogr., Sect. C* **57** 1234 (2001)
42. N Segal, J F Vente, T S Bush, P D Battle *J. Mater. Chem.* **6** 395 (1996)
43. S Frenzen, Hk Müller-Buschbaum *Z. Naturforsch., B* **51** 225 (1996)
44. C Lampe-Onnerud, M Sigrist, H-C zur Loye *J. Solid State Chem.* **127** 25 (1996)
45. M J Davis, M D Smith, K E Sütizer, H-C zur Loye *J. Alloys Compd.* **351** 95 (2003)
46. S Frenzen, Hk Müller-Buschbaum *Z. Naturforsch., B* **51** 1204 (1996)
47. S Frenzen, Hk Müller-Buschbaum *Z. Naturforsch., B* **50** 581 (1995)
48. C A Moore, E J Cussen, P D Battle *J. Solid State Chem.* **153** 254 (2000)
49. S Niitaka, H Kageyama, M Kato, K Yoshimura, K Kosuge *J. Solid State Chem.* **146** 137 (1999)
50. K E Stitzer, W H Henley, J B Claridge, H-C zur Loye, R C Layland *J. Solid State Chem.* **164** 220 (2002)
51. R C Layland, S L Kirkland, P Núñez, H-C zur Loye *J. Solid State Chem.* **139** 416 (1998)
52. R C Layland, S L Kirkland, H-C zur Loye *J. Solid State Chem.* **139** 79 (1998)
53. B A Reisner, A M Stacy *J. Am. Chem. Soc.* **120** 9682 (1998)
54. C Dussarrat, J Fompeyrine, J Darriet *Eur. J. Solid State Inorg. Chem.* **32** 3 (1995)
55. J B Claridge, H-C zur Loye *Chem. Mater.* **10** 2320 (1998)
56. H-C zur Loye, K E Stitzer, M D Smith *Inorg. Chem.* **40** 5152 (2001)
57. K E Stitzer, M D Smith, J Darriet, H-C zur Loye *Chem. Commun.* 1680 (2001)
58. K E Stitzer, A El Abed, J Darriet, H-C zur Loye *J. Solid State Chem.* **177** 1405 (2004)
59. T Shishido, K Ukei, T Fukuda *J. Alloys Compd.* **237** 89 (1996)
60. H Fjellvåg, E Gulbrandsen, S Aasland, A Olsen, B C Hauback *J. Solid State Chem.* **124** 190 (1996)
61. F Abraham, S Minaud, C Renard *J. Mater. Chem.* **4** 1763 (1994)
62. M Huve, C Renard, F Abraham, G Van Tendeloo, S Amelinckx *J. Solid State Chem.* **135** 1 (1998)
63. J A Campá, E Gutiérrez-Puebla, M A Monge, I Rasines, C Ruíz-Valero *J. Solid State Chem.* **108** 230 (1994)
64. W T A Harrison, S L Hegwood, A J Jacobson *J. Chem. Soc., Chem. Commun.* 1953 (1995)
65. G V Bazuev, V G Zubkov, V N Krasil'nikov, K N Mikhalev, T I Arbuzova *Dokl. Akad. Nauk* **363** 634 (1998) [a]
66. E J Cussen, J F Vente, P D Battle *J. Am. Chem. Soc.* **121** 3958 (1999)
67. S Kawasaki, M Takano, T Inami *J. Solid State Chem.* **145** 302 (1999)
68. G V Bazuev, V G Zubkov, I F Berger, in *Solid State Chemistry 2000 (Book of Abstracts), Prague, 2000* p. 22
69. G V Bazuev, V G Zubkov, I F Berger, T I Arbuzova *Solid State Sci.* **1** 365 (1999)
70. G V Bazuev, V G Zubkov, I F Berger, T I Arbuzova *Zh. Neorg. Khim.* **45** 1204 (2000) [b]
71. V G Zubkov, G V Bazuev, A P Tyutyunnik, I F Berger *J. Solid State Chem.* **160** 293 (2001)
72. V G Zubkov, A P Tyutyunnik, I F Berger, G V Bazuev *Dokl. Akad. Nauk* **376** 347 (2001) [a]
73. M D Smith, H-C zur Loye *Chem. Mater.* **12** 2404 (2000)
74. M James, J P Attfield *Chem. – Eur. J.* **2** 737 (1996)
75. M D Smith, J K Stalick, H-C zur Loye *Chem. Mater.* **11** 2984 (1999)
76. G Wehrum, R Hoppe *Z. Anorg. Allg. Chem.* **617** 45 (1992)
77. P D Battle, S J Hartwell, C A Moore *Inorg. Chem.* **40** 1716 (2001)
78. V A Carlson, A M Stacy *J. Solid State Chem.* **96** 332 (1992)
79. E Cuno, Hk Müller-Buschbaum *Z. Anorg. Allg. Chem.* **572** 175 (1989)
80. K Boulahya, M Parras, J M González-Calbet *J. Solid State Chem.* **145** 116 (1999)
81. G V Bazuev, V N Krasil'nikov, D G Kellerman *J. Alloys Compd.* **352** 190 (2003)
82. G V Bazuev, V G Zubkov, V N Krasil'nikov, in *Khimiya, Tekhnologiya i Promyshlennaya Ekologiya Neorganicheskikh Soedinenii (Sbornik Nauchnykh Trudov), Perm', 2001* [The Chemistry, Technology and Industrial Ecology of Inorganic Compounds (Collection of Scientific Works), Perm', 2001] No. 4, p. 120
83. A El Abed, E Gaudin, J Darriet *Acta Crystallogr., Sect. C* **58** 138 (2002)
84. G V Bazuev, D G Kellerman *Zh. Neorg. Khim.* **47** 1772 (2002) [b]
85. A El Abed, E Gaudin, S Lemaux, J Darriet *Solid State Sci.* **3** 887 (2001)
86. A El Abed, E Gaudin, J Darriet, M-H Whangbo *J. Solid State Chem.* **163** 513 (2002)
87. M A Melkozerova, G V Bazuev *Zh. Neorg. Khim* **49** 1925 (2004) [b]
88. K Boulahya, M Parras, J M Gonzáles-Calbet, J L Martinez *Chem. Mater.* **15** 3537 (2003)
89. G V Bazuev, N A Zaitseva, V N Krasil'nikov, D G Kellerman *Zh. Neorg. Khim* **48** 219 (2003) [b]
90. M Hernando, K Boulahya, M Parras, J M González-Calbet *Eur. J. Inorg. Chem.* 3190 (2002)

91. P D Battle, J C Burley, E J Cussen, J Darriet, F Weill *J. Mater. Chem.* **9** 479 (1999)
92. M Hernando, K Boulahya, M Parras, J M González-Calbet, U Amador *Eur. J. Inorg. Chem.* 2419 (2003)
93. G V Bazuev, N A Zaitseva, D G Kellerman *Solid State Sci.* **5** 1465 (2003)
94. K Boulahya, M Parras, J M González-Calbet *J. Solid State Chem.* **142** 419 (1999)
95. G V Bazuev, N A Zaitseva, D G Kellerman *Zh. Neorg. Khim* **49** 361 (2004) [b]
96. G V Bazuev, N A Zaitseva, V N Krasil'nikov *Zh. Neorg. Khim* **47** 1418 (2002) [b]
97. K Boulahya, M Parras, J M González-Calbet, J L Martinez *Chem. Mater.* **16** 5408 (2004)
98. N A Jordan, P D Battle, S van Smaalen, M Wunschel *Chem. Mater.* **15** 4262 (2003)
99. A El Abed, S E Elgebbaj, M Zakhour, M Champeaux, J M Perez-Mato, J Darriet *J. Solid State Chem.* **161** 300 (2001)
100. J Darriet, L Elcoro, A El Abed, E Gaurdin, J M Perez-Mato *Chem. Mater.* **14** 3349 (2002)
101. O Gourdon, V Petricek, M Dusek, P Bezdicka, S Durovic, D Gyepesova, M Evain *Acta Crystallogr., Sect. B* **55** 841 (1999)
102. A S Aldridge, P D Battle, J S O Evans, C A Moore, T J Prior, P J Wiseman *Inorg. Chem.* **44** 197 (2005)
103. E Quarez, P Roussel, O Perez, H Leligny, A Bendraoua, O Mentre *Solid State Sci.* **6** 931 (2004)
104. N A Zaitseva, V N Krasil'nikov, G V Bazuev, G Sh Shekhtman, T I Chupakhina *Izv. Akad. Nauk, Ser. Fiz.* **68** 731 (2004) [c]
105. M Strunk, Hk Müller-Buschbaum *J. Alloys Compd.* **209** 189 (1994)
106. R Kriegel, A Feltz, L Walz, A Simon, H-J Mattausch *Z. Anorg. Allg. Chem.* **617** 99 (1992)
107. R D Shannon *Acta Crystallogr., Sect. A* **32** 751 (1976)
108. Y Bréard, C Michel, A Maignan, B Raveau *Solid State Commun.* **118** 517 (2001)
109. G M Veith, I D Fawcett, M Greenblatt, M Croft, I Nowik *Int. J. Inorg. Mater.* **2** 513 (2000)
110. T I Chupakhina, G V Bazuev, N A Zaitseva *Zh. Neorg. Khim* **49** 725 (2004) [b]
111. H Kageyama, K Yoshimura, K Kosuge, M Azuma, M Takano, H Mitamura, T Goto *J. Phys. Soc. Jpn.* **66** 3996 (1997)
112. S Majumdar, V Hardy, M R Lees, D M Paul, H Rousseliere, D Grebille *Phys. Rev. B* **69** 024405 (2004)
113. S Rayaprol, E V Sampathkumaran *Phys. Rev. B* **71** 094403 (2005)
114. A Niazi, E V Sampathkumaran, P L Paulose, D Eckert, A Handstein, K-H Müller *Phys. Rev. B* **65** 064418 (2002)
115. S H Iron, T D Sangrey, K M Beauchamp, M D Smith, H-C zur Loye *Phys. Rev. B* **61** 11594 (2000)
116. A Niazi, E V Sampathkumaran, P L Paulose, D Eckert, A Handstein, K-H Müller *Solid State Commun.* **120** 11 (2001)
117. S Rayaprol, K Sengupta, E V Sampathkumaran *Phys. Rev. B* **67** 180404 (R) (2003)
118. S Niitaka, K Yoshimura, K Kosuge, M Nishi, K Kakurai *Phys. Rev. Lett.* **87** 177202 (2002)
119. M-H Whangbo, D Dai, H-J Koo, S Jobic *Solid State Commun.* **125** 413 (2003)
120. V Hardy, M R Lees, A Maignan, S Hebert, D Flahaut, C Martin, D M Paul *J. Phys.: Condens. Matter* **15** 5737 (2003)
121. S Rayaprol, K Sengupta, E V Sampathkumaran, Y Matsushita *J. Solid State Chem.* **177** 3270 (2004)
122. J F Vente, J K Lear, P D Battle *J. Mater. Chem.* **5** 1785 (1995)
123. J N Mwamuka, W R Gemmill, K E Stitzer, M D Smith, H-C zur Loye *J. Alloys Compd.* **377** 91 (2004)
124. S Rayaprol, K Sengupta, E V Sampathkumaran *Solid State Commun.* **128** 79 (2003)
125. K Sengupta, S Rayaprol, K K Iyer, E V Sampathkumaran *Phys. Rev. B* **68** 012411 (2003)
126. E V Zabolotskaya, L V Zolotukhina, N A Zaitseva, G V Bazuev *Zh. Neorg. Khim* **48** 1527 (2003) [b]
127. L V Zolotukhina, E V Zabolotskaya, G V Bazuev *Zh. Fiz. Khim.* **78** 1895 (2004) [d]

[a] — *Dokl. Chem. (Engl. Transl.)*
[b] — *Russ. J. Inorg. Chem. (Engl. Transl.)*
[c] — *Bull. Russ. Acad. Sci., Phys. (Engl. Transl.)*
[d] — *Russ. J. Phys. Chem. (Engl. Transl.)*